Available online at www.sciencedirect.com
SCIENCE DIRECT
ELSEVIER
Icarus 174 (2005) 336–359
ICARUS
www.elsevier.com/locate/icarus

High latitude patterned grounds on Mars: Classification, distribution and climatic control

Nicolas Mangold *

Laboratoire IDES-Orsay, Université Paris-Sud, CNRS, Bat. 509, 91405 Orsay, France

Received 19 January 2004; revised 8 June 2004

Available online 26 January 2005

Abstract

Patterned grounds such as polygonal features and slope stripes are the signature of the presence of ground ice and of temperature variations in cold regions on Earth. Identifying similar features on Mars is important to understand its past climate as well as the ground ice distribution. In this study, young patterned grounds are classed and mapped from the systematical analysis of Mars Observer Camera high resolution images. These features are located poleward of 55° latitude which fits the distribution of ground ice found by the Neutron Spectrometer onboard Mars Odyssey. Thermal contraction due to seasonal temperature variations is the predominant process of formation of polygons formed by cracks which sizes vary from 15 to 300 m. The small (<40 m) widespread polygons are very recent and degraded by the desiccation of ground ice from the cracks which enhances the effect of ice sublimation. The large polygons (50 to 300 m) located only around the south CO_2 polar cap indicate the presence of ground ice and thus outline the limit of the CO_2 ice cap. They could be due to the blanketing of water ice deposits by the advances and retreats of the residual CO_2 ice cap during the last thousand years. Large (50–250 m) and homogeneous polygons similar to ice wedge polygons, hillslope stripes and solifluction lobes may indicate that specific environments such as crater floors and hillslopes could have been submitted to freeze–thaw cycles, possibly related to higher summer temperatures in periods of obliquity higher than 35°. These interpretations must be strengthened by higher resolution images such as those of the HiRise mission of the Mars Reconnaissance Orbiter because locations with past seasonal thaw could be of major interest as potential landing sites for the Phoenix mission.
© 2004 Elsevier Inc. All rights reserved.

Keywords: Mars; Geological processes; Ice; Water

1. Introduction

The occurrence of polygons on Mars similar to those found on Earth in periglacial regions has been the subject of debates for three decades. Large polygonal systems were identified on Viking images of the Northern plains (Pechmann, 1980; Lucchitta, 1983). These polygons, 2–10 km across with bounding through widths of 200 to 800 m, are too large to be compared to terrestrial periglacial polygons and could be better related to tectonic stresses, maybe in relation with a past ocean (Hiesinger and Head, 2000). New high resolution images of the Mars Observer Camera (MOC) of MGS show small-scale polygons much more similar in size to terrestrial patterned ground (Baker, 2001; Malin and Edgett, 2001; Masson et al., 2001; Yoshikawa, 2002; Mangold et al., 2002a, 2003; Kuzmin et al., 2002, 2003; Leverington, 2003). Polygons found in the Utopia and Elysium regions are several hundreds of meters large and could correspond to Late Amazonian events of thermal cracking and a possible control by thawed ground ice (Seibert and Kargel, 2001). Nevertheless, the preferred orientation of cracks suggests a control by tectonic stresses (Yoshikawa, 2002). Such interpretations question the origin of small scale polygons as due to periglacial processes created by the temperature variations in ice rich layers. Identifying polygons related to periglacial processes is important in order to study recent modifications of ice distribution and climate on Mars.

* Fax: +33-1-6019-1446.
E-mail address: mangold@geol.u-psud.fr.

0019-1035/$ – see front matter © 2004 Elsevier Inc. All rights reserved.
doi:10.1016/j.icarus.2004.07.030

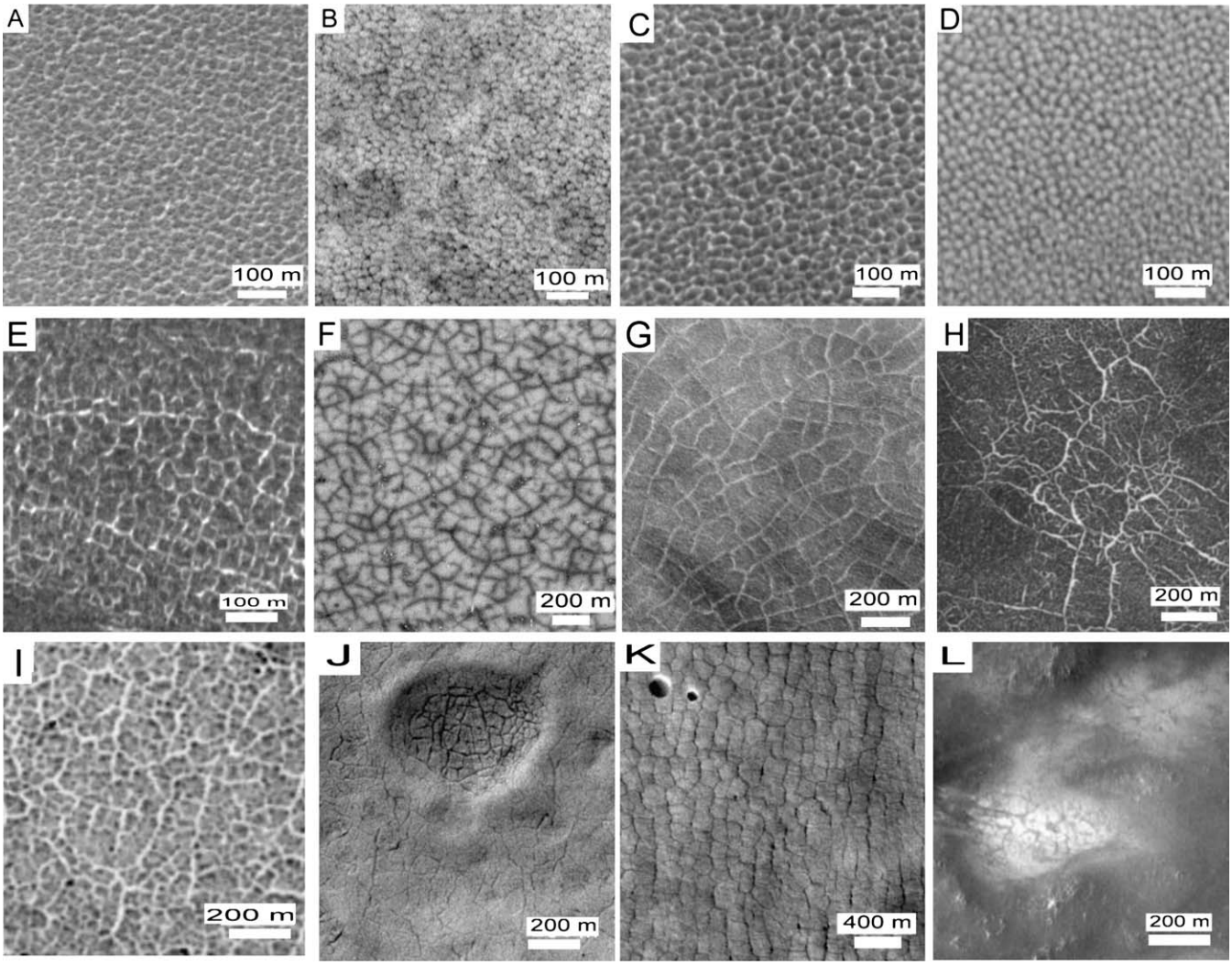

Fig. 1. Different types of small scale patterned grounds on Mars. (A) Homogeneous small polygons without apparent cracks. MOC image #M02-04505, 65.7° S, 176.8° W, $L_s = 162°$ (L_s = solar longitude). (B) Regular hexagonal patterns. MOC image #M04-02503, 63.2° S, 275.4° W, $L_s = 192.5°$. (C) Similar to (A) in the northern hemisphere. MOC image #M14-00154, 60.6° N, 2.9° W, $L_s = 329.1°$. (D) Hummocky terrains. MOC image #M03-04266, 54.1° S, 229.5° W, $L_s = 174.9°$. (E) Small cracks visible from the presence of CO_2 ice inside. MOC image #M08-03679, 69° S, 98.4° W, $L_s = 225.9°$. (F) Straight cracks close to south polar cap. MOC image #M09-01292, 84.9° S, 103.6° W, $L_s = 238.4°$. (G) Ice wedge like polygons on the floor a 20 km diameter crater in the northern hemisphere. MOC image #E03-00299, 64.7° N, 292.9° S, $L_s = 140.6°$. (H) Complex networks of cracks defining polygons of different sizes. MOC image #M08-05725, 67.7° S, 347.7° W, $L_s = 230.2°$. (I) Polygons of variable size with fractal like geometry. MOC image #M09-04469, 74.4° S, 98.9° W, $L_s = 246°$. (J) Cracks after complete defrosting of CO_2 ice. MOC image #M12-00012, 69.6° S, 271.4° W, $L_s = 293.2°$. (K) 300 m large polygons of Utopia Planitia. MOC image #M04-01631, 44.3° N, 272,7° W, $L_s = 190°$. (L) Polygons localized inside bright areas in depression patch in the equatorial region near Schiapparelli basin. MOC image #AB102306, 5.4° S, 340.7° W, $L_s = 201°$.

In this study, polygons 15 to 300 m large (Fig. 1) found at high latitudes of Mars are described and classified. The classification uses criteria such as the size of the polygons, their homogeneity of their size, the occurrence of cracks and the control by local topography. The results show that most patterned grounds can be classified into nine types. Four types are restricted to high latitudes of the southern hemisphere. Clearly associated with climatic variations are the four types of polygons found at the same latitudes on both hemispheres. Scenarios of their formation is proposed, invoking as a major process seasonal thermal contraction. The role of a potential freeze–thaw cycles is finally discussed for some of these landforms.

2. Classification, distribution and age of patterned grounds on Mars

2.1. Description of martian patterned grounds and terrestrial analogs

Small-scale patterned grounds on Mars display a large variety of geometry and size. A common kind of patterned ground consists of very regularly spaced polygons, typically 30 m large, apparently devoid of straight cracks (Figs. 1A, 1C). Similar patterns can be found in both hemispheres (Fig. 1C). Such small patterns were identified by Malin and Edgett (2000) (Fig. 9b at 54,8° S) in the vicinity of recent

gullies. On Fig. 1B, polygons are slightly smaller (25 m) but very homogeneous and more hexagonal. Another difference is that the polygon borders are bright in Figs. 1A and 1C but dark in Fig. 1B. Bright borders can be explained by CO_2 frost trapped in the trough between polygons, in agreement with the season (late winter or spring) at which the images were taken. By contrast, the dark borders of polygons of Fig. 1B can be due either to differences in material albedo, or to shadows due to troughs between polygons. In the case of Fig. 1D, the dark bounds are certainly due to shadows rather than differences in composition, resulting in a texture formed by hummocks. Patterns such as Fig. 1D have been described as "basket ball terrain" by Head et al. (2003), though it is not clear if this term includes also small patterns such as Figs. 1A–1C.

Straight troughs define polygons in the range of 20 to 400 m in width forming crack networks of a very different geometry (Figs. 1E–1L). On Figs. 1E, 1G, 1H, and 1I, networks of cracks are outlined by the presence of carbonic ice frost which suggests bounding troughs separating polygons (Kossacki and Markiewicz, 2002). The identification of bounding troughs is also possible from their shadows after the seasonal CO_2 ice is gone (Fig. 1J). On Fig. 1F located close to the south polar cap, it is not clear why cracks appear dark, but it may indicate differences in seasonal ice thickness over the bounding troughs. The Utopia basin region (40° N) displays MOC images with regular sized polygons usually two times larger than the largest polygons in regions of high latitudes (Fig. 1K). Polygons in equatorial regions are very sparse and have a geometry different than the cracks of the high latitude regions (Fig. 1L).

All the described patterned grounds have different organizations that may correspond to different processes of formation. On Earth, the formation of patterned ground in cold regions is mainly due to (1) freeze–thaw cycles and/or (2) thermal contraction of ground ice (Johnston, 1981; French, 1996). Nevertheless, similar patterns can exist independently of the periglacial context as a consequence (3) of the desiccation of wet sediments or (4) of tectonic stresses.

Freeze–thaw cycles create features like sorted stripes on slopes, sorted circles, sorted nets and sorted polygons (Figs. 2A, 2B), mud boils or hummocks (Fig. 2D). All of these landforms involve processes due to the ice/liquid water transition phase (French, 1996). These physical processes may correspond to thermally-driven convection, diapirism, or differential frost heave and ice segregation (Ray et al., 1983; Gleason et al., 1986; Hallet and Prestrud, 1986; Swanson et al., 1999; Van Vliet-Lanoë, 1991; Fowler and Krantz, 1994; Kessler and Werner, 2003). The other main type of terrestrial patterned ground is characterized by networks of cracks, also called non-sorted nets or more simply polygons. In cold regions, cracks are due to the thermal contraction of the ground ice during winter (Figs. 2C, 2D). No seasonal thaw of ground ice is needed for thermal contraction, but, on Earth, cracks are often filled by water coming from the melting of snow or ground ice which freezes inside the cracks in winter and forms the so-called ice wedge (Lachenbruch, 1962; French, 1996; Plug and Werner, 2001). In that case specific landforms like mudboils (Fig. 2D) or ridges over cracks (Fig. 2D) can occur in conjunction with thermal contraction. Some of those observed on Mars (Figs. 1G, 1F) have a geometry very similar to terrestrial ice wedge polygons (Figs. 2C, 2D).

The desiccation of muddy sediments (Fig. 2E) or specific tectonic stresses (Hiesinger and Head, 2000) can form networks of cracks with a geometry very similar to those formed by thermal contraction. None of the polygons observed seem to correspond to mud cracks, with the possible exception of Fig. 1L which shows cracks localized inside a bright depression that could be interpreted as ancient lake deposits. In cold regions, desiccation cracks can also form as a consequence of seasonal thaw. Van Vliet-Lanoë (1998) describes different kind of cryoturbation with features like cracks formed by desiccation due to the groundwater flows subsequent to the formation of sorted polygons. Geomorphic arguments are thus not always sufficient to distinguish between all possible processes forming polygonal features. For this reason, all images of recent patterned grounds on Mars are classed in different types in order to highlight possible indicators of the processes involved.

2.2. *Criteria used for the classification*

The systematic studies of patterned grounds, i.e., regular polygons, circles or stripes, on the entire Mars was done using MOC images M01 to E06 with a resolution better than 6 m/pixel. These data cover more than one martian year, so that both hemispheres are equitably covered. Dissected terrains which cover many mid-latitude regions of Mars (Mustard et al., 2001) are not included because they do not display a regular texture like the polygons. The area covered by patterned grounds on each MOC image is also taken in account in the classification because small isolated patches of polygons on one MOC image could correspond to local effects. Images which surface is covered by roughly 5% or less of patterned grounds are not included in the classification. For example, Fig. 1L was not included in the mapping because the image only shows a small patch of polygons.

The interpretation of patterned ground is also complicated by the presence of features of very different ages. Thus, only very young features are included in the classification. The age is difficult to determine because only small impact craters can be used but most MOC images containing patterned ground are completely devoid of fresh craters (Fig. 1). On the contrary, polygons of the Athabasca Valles region (10° N, 200° W) are impacted significantly so that they are not included. Polygons of Utopia and Elysium regions located in a latitude range of 40°–50° (Seibert and Kargel, 2001; Kuzmin et al., 2002), although sparsely impacted, show 100 m large craters on several images (Fig. 1K). Despite being very recent (Late Amazonian), they still seem to be significantly older than the polygons of this

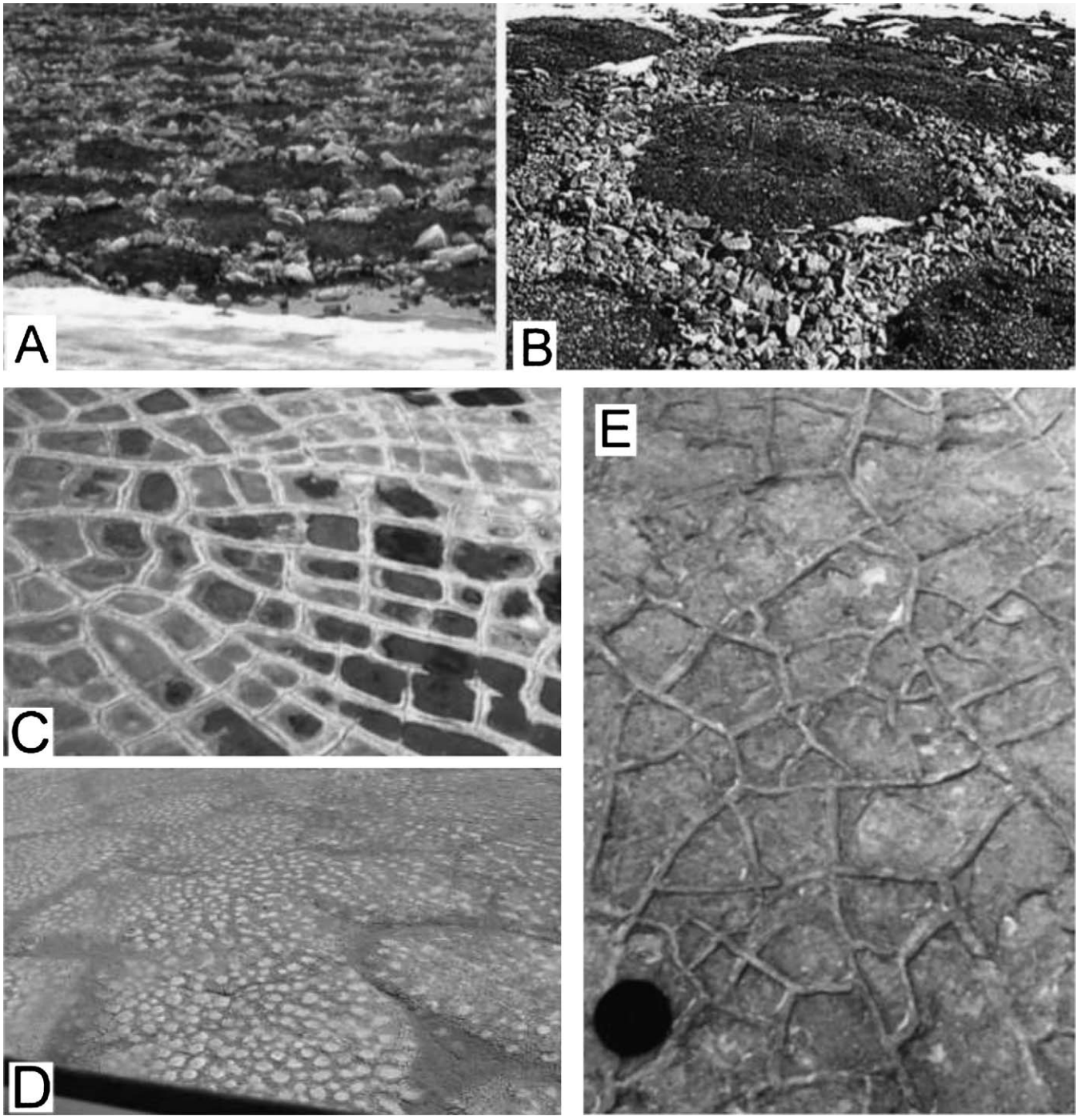

Fig. 2. Different types of patterned ground on Earth. (A) About 1 m large sorted polygons in Greenland (70° N), Inugsukajik. Photograph J.-P. Peulvast. (B) Unusually large sorted polygons of 20 m. Rocks on the border are up to 1 m large in Ellesmere Island (77° N). GSC photograph #2002-278. (C) About 30 m large ice-wedge polygons in Nunavut, Canada. Notice the presence of ridges bordering cracks. GSC photograph. (D) Ice-wedge polygons in Howe island, Alaska. Notice the presence of small hummocks inside polygons which are mud boils 1–2 m large. Photo Skip Walker, Univ. of Alaska Fairbanks. (E) About 10 cm large fossil desiccation cracks in Precambrian sandstones, Mauritania. Photograph N. Mangold.

study and are not included mainly for this reason. Nevertheless, these polygons are geologically recent and interesting for the understanding of past climate changes (Seibert and Kargel, 2001).

After this first step, all MOC images showing periodically patterned ground are classed using four main criteria.

1. *Their homogeneity in size*: Polygons are listed as "homogeneous" polygons if they have a regular width and as "variable" in the opposite case. For example, polygons are heterogeneous if they range from 20 to 200 m in width on the same image. The homogeneous group is limited to images in which the largest polygons are no more than 3 times

wider than the smallest. For example, 20 m for the smallest compared to 60 m for the largest, is at the transition between homogeneous and "variable" sizes. By comparison, terrestrial polygons are usually homogeneous.

2. *Their absolute sizes*: The width of polygons is an important criterion in identifying the mechanism, because the width is related to the thickness affected by thermal cracks. In the case of homogeneous widths, polygons are listed as "Small" if they are less than 40 m wide and as "Large" if they are more than 40 m wide, despite they are still smaller than 500 m. The limit at 40 m is justified a posteriori because it separates different types of features. Notice that the large polygons refer to features that are still much smaller than the giant polygons of the northern plains which are a few kilometers across.

3. *The identification of cracks and the type of crack networks*: Cracks are identified from the linear outlines of bounding troughs. Classes A, B, and C are defined for cracks corresponding respectively to random orthogonal, oriented orthogonal and hexagonal patterns (Fig. 3). Hexagonal patterns (class C) with angular intersections of 120° form when frost cracks develop at a series of points and that each crack develops more or less simultaneously (French, 1996). This case could reflect the homogeneity of the subsurface and of the cooling rate (French, 1996). The random orthogonal pattern (class A) is thought to infer an evolutionary sequence in which primary frost cracks develop in an essentially random pattern (Fig. 3A). These first segments of fractures locally reduce the tensile stress in the ground on a line perpendicular to the fracture. So, secondary cracks form preferentially on lines orthogonal to the primary cracks forming a T-shaped intersection (e.g., Plug and Werner, 2002). Such a system is listed as random orthogonal in contrast to the oriented orthogonal systems (class B) which often occurs on Earth in the vicinity of standing bodies of water (Lachenbruch, 1966; French, 1996). Kuzmin et al. (2002) distinguish cracks by their intersections in either 3-rays or 4-rays. Using this nomenclature, hexagonal polygons (class C) would contain 3-rays only, oriented orthogonal systems (class B) would be dominated by 4-ray intersections, while random orthogonal polygons (class A) would contain a similar proportion of 3-ray and 4-ray intersections.

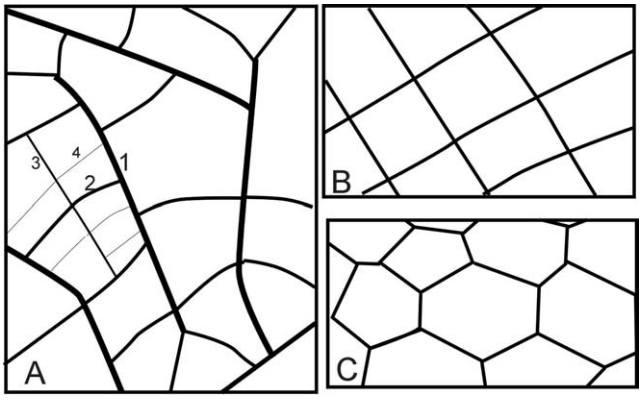

Fig. 3. (A) Random orthogonal network of cracks. (B) Rectangular network. (C) Hexagonal network (adapted from French, 1996).

4. *The presence of a topographic control*: Patterned grounds are sometimes systematically associated with topography such as crater interiors or hillslopes. Other landforms not correlated to topography are observed on flat plains or on hilly materials without apparent control of the cracks direction by the topography. The particular case of slope stripes on hillslopes is developed in a specific section.

Using these criteria the patterned grounds of 548 images can be listed in eight main types (Table 1). Other classifications can be relevant depending on the selection of criteria and upcoming high resolution images might reveal more types of patterned ground. This classification is a more detailed classification than the four types proposed in Mangold et al. (2004). A total of 15 images with cracks forming incomplete networks are grouped in the Miscellaneous type M. They can be due either to cracks formed by a volumetric contraction not strong enough to complete polygons, or erosion of some of the cracks or unusual geometry not seen in other locations. They are not discussed in the following because their geometry does not give any information about their formation.

2.3. Geographic distribution of patterned ground

Four types of polygons are located in both hemispheres at the same latitudes (Fig. 4) indicating climate effects. Images with small S1 crack networks are in very low number (33) compared to the images containing S2 polygons (151) and S3 hummocks (250). The ratio of images in the North and the South (3/4 in the south) could be a result of sampling effects because northern plains are often covered by haze. Types S2 and S3 have been separated by a dashed line in Table 1 because they were difficult to separate. There seems to be a continuity from rounded hummocks to polygonal shapes. The type S1 displays cracks and it is more sparsely distributed by comparison to types S2 and S3. Nevertheless, the maximum number of polygons is shifted in latitude from S3 to S1 on the histogram (Fig. 5A). The type S3 occurs mainly between 54° and 60° latitude whereas the type S2 becomes dominant between 63° and 69° latitude and S1 is dominant between 72° and 75° latitude. Thus, S1 could also be a continuity of S3 and S2. On the other hand, the average size of small polygons apparently increase in sizes from 52° to 70° latitude (Fig. 5B).

There are only two classes of large and homogeneous polygons. The first class LT is found in close connection to topographic features such as craters and hillslopes (Fig. 1G). Polygons LT are located between 50° and 75° latitude in both hemispheres with a maximum around 65° in both hemispheres, thus at the same latitudes as the small polygons but in a much more restricted proportion. The second class LPC (Fig. 1F) is located around the south polar cap (Fig. 4). No type of large homogeneous polygons seem to exist outside

Table 1
Classification of patterned grounds on Mars

Size		Type	Number of images	Characteristics	Crack class	Examples
Homogeneous size						
Large (>40 m)	50–250 m	LT	NH = 14 SH = 26	Large polygons connected to topography (craters, hillslopes)	B > A no C	Figs. 1G, 9, 10, 11
	40–250 m	LPC	NH = 0 SH = 19	Large polygons around polar cap	A ≫ C no B	Figs. 1F, 12
Small (<40 m)	15–50 m	S1	NH = 13 SH = 20	Small polygons with cracks	A > B > C	Fig. 1E
	15–40 m	S2	NH = 36 SH = 115	Small polygons (homogeneous texture with polygonal shapes)	No cracks	Figs. 1A, 1B, 1C, 7B
	10–30 m	S3	NH = 78 SH = 172	Hummocky terrains (homogeneous texture with round shaped features)	No cracks	Figs. 1D, 7A, 12
Variable size	10 to 200 m	VF	NH = 0 SH = 24	Fractal crack networks (crack width decreases with size)	A > B > C	Fig. 1I
	15 to 200 m	VV	NH = 0 SH = 9	Very variable size (same crack width)	A ∼ B, no C	Fig. 1J
	10 to 150 m	VCX	NH = 0 SH = 7	Complex assemblages of cracks (Fractal + irregular)	A > B > C	Fig. 1H
Miscellaneous		M	NH = 3 SH = 12	Incomplete crack networks, dendritic cracks or parallel cracks without full shape of polygons		

NH = North Hemisphere. SH = South Hemisphere. See text for details. Crack class: A = Random orthogonal, B = Orthogonal, C = Hexagonal. Type LT = Large and influenced by Topography. LPC = Large around Polar Cap. S1 to S3 are Small. VF = Variable with fractal shape. VV = Variable without organization. VCX = Variable and complex, M = Miscellaneous.

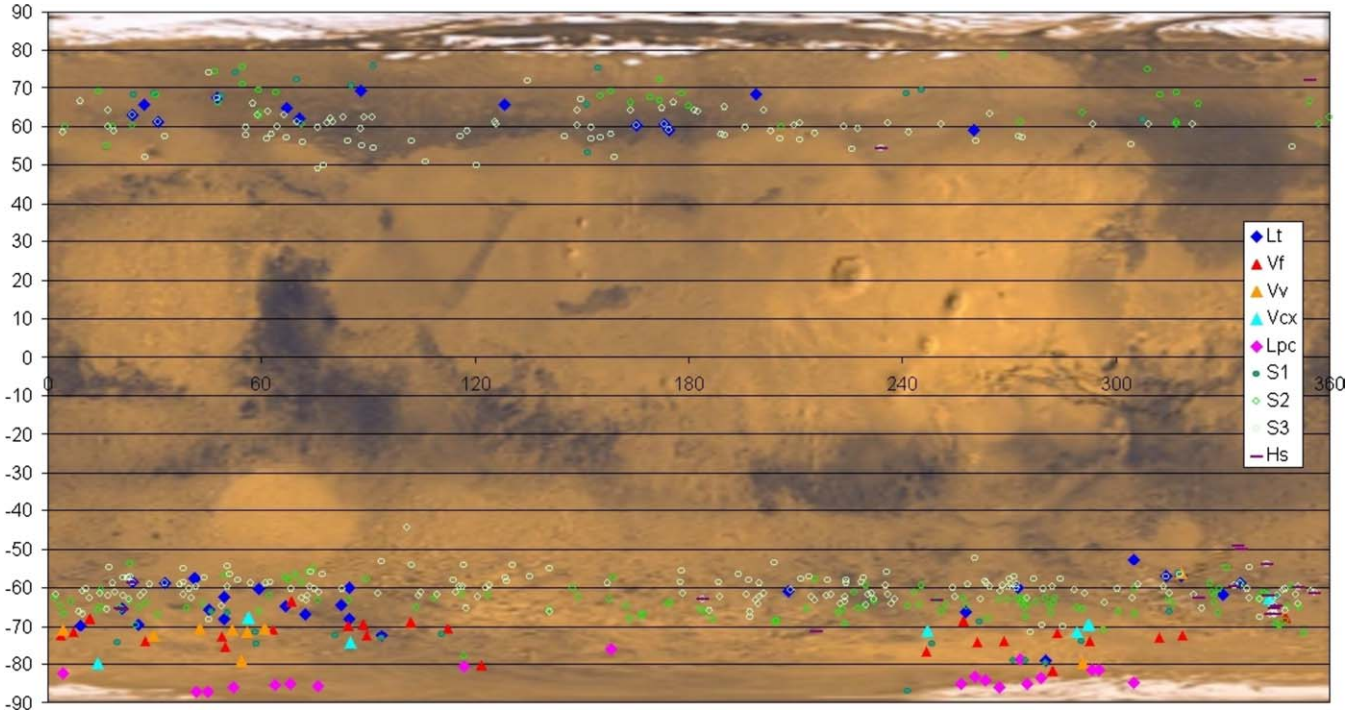

Fig. 4. Distribution of patterned ground on Mars from MOC images M01 to E06. The background shows a mosaic of MOC wide angle images with Tharsis hemisphere at right (Eastward longitudes). LPC polygons are close to south polar cap at longitude especially around 270° E. There is a strong limit at 55° of latitude.

these two groups, except large polygons geographically restricted to Elysium and Utopia (Seibert and Kargel, 2001).

The polygons of variable sizes are split in three groups named fractal (type VF), very variable (type VV) and complex (type VCX) which consist of a total number of 38 images. Fractal networks VF (Fig. 1I) display a fractal geometry with cracks decreasing in size and width like on Fig. 3A. In contrast, the geometry of the VV type is very heterogeneous without hierarchy in the width of cracks. The discrimination between these two end members is difficult on many images and the most complex ones are classed as complex VCX (Fig. 1H). The distribution of all V types is restricted

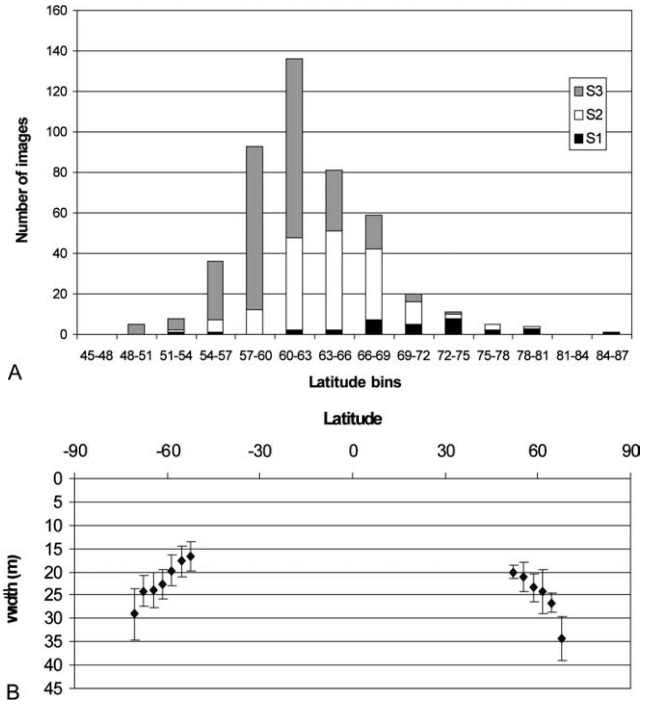

Fig. 5. (A) Histogram of latitudes versus number of polygons types S1, S2, and S3. Latitudes are grouped by 3° bins cumulated over the two hemispheres. Distinct graph for each hemisphere would give the same result. The total maximum occurs around 60° but the relative maximum of each class is shifted from 57° for S3 to 72° for S1. (B) Size of polygons S2 + S3 versus latitude. The size is an average of all features over the 3° latitude bins of figure (A). The error bars show the standard deviation. The size is probably overestimated because the smallest patterns are under the resolution of MOC images.

to the southern hemisphere at latitudes between 55° and 80° with a maximum near 70°. They do not depend on the local topography and they present different classes of cracks with class A (random orthogonal) strongly dominant. Polygons of variable sizes are also more regionally grouped. There is a gap of such cracks in regions located between longitudes 120° E and 240° E.

2.4. Description and distribution of slope stripes and striated soils

Several MOC images show a type of patterned ground which consists of stripes located on hillslopes. On Earth, slope stripes are due to processes involving freeze–thaw cycles (Werner and Hallet, 1993). A first type of terrestrial stripes corresponds to sorted polygons on flat plateaus (Figs. 6A, 6B) which become progressively sorted stripes on gentle slopes (Washburn, 1956; Goldthwait, 1976; Ballantyne, 1996). These stripes are related to the processes that create sorted polygons like the elongation of convection cells, diapirs in the direction of the slope or lateral squeezing of rocks perpendicular to the slope (Krantz, 1990; Kessler and Werner, 2003; Peterson and Krantz, 2003). A second group of terrestrial stripes exist without connections to polygons on flat plateaus (Fig. 6C). These stripes are explained by processes implying ice segregation like ice needles (Werner and Hallet, 1993) or solifluction (French, 1996). However, many stripes are complex and what dictates the spacing on such terrestrial stripes unrelated to polygons is still unclear (Francou et al., 2001).

Some MOC images show regular patterns of polygons transforming into stripes on gentle slopes (Figs. 7A, 7B). On Fig. 7A, the stripes follow the main slopes and become polygons at the foothill. On Fig. 7B, the transition between polygons and stripes occurs on a gentle slope like in terrestrial examples (Fig. 6B) though no measurements of this slope were possible using MOLA (Mars Observer Laser Altimeter) data. Other MOC images show the occurrence of regular stripes on the flanks of hillslopes without association with polygons which can be compared to the second type of terrestrial stripes (Figs. 7C, 7D). On these two images, stripes are periodic and of constant width therefore being very different from any mass wasting features such as dark slope streaks that cover some of the equatorial regions (Sullivan et al., 2001). Slopes measured from MOLA profiles have gradients of 5° in Fig. 7C and 7° in Fig. 7D. Such gradients are consistent with those where stripes are found which can vary from 3° to 20° (French, 1996; Francou et al., 2001).

Stripes about 50 m large found by Malin and Edgett (2001) in plains of the northern hemisphere are not comparable to hillslopes stripes because they occur on flat plains without any correlation with the slope. Rough stripes observed on hillslopes at 40°–50° latitude were interpreted as possible sorted stripes (Cabrol and Grin, 2002), but their association with nearby viscous features makes gravity-driven processes due to icy viscous flows without the involvement of freeze–thaw cycles more likely (Milliken et al., 2003). These two types of stripes are not included in the distribution.

Hillslopes stripes (type Hs) are located in the same range of latitudes between 55° and 75° like other kind of polygons (Hs on Fig. 4). They are more abundant in the southern hemisphere (17 Hs) than in the northern one (2 Hs) which is probably a consequence of the rougher topography of the southern hemisphere compared to the northern plains (Kreslavsky and Head, 2003a). In summary, stripes are interesting features to take into account in the understanding of patterned ground on Mars as they often indicate features related to cyclic thaw but their limited number and their small sizes may reduce the validity of the interpretation.

2.5. Relations of patterned ground with ground ice and surface properties

The distribution of patterned grounds can be correlated to the distribution of near-surface ice found by the Neutron Spectrometer (NS) of the Gamma-Ray Spectrometer (GRS) onboard Mars Odyssey (Mangold et al., 2003, 2004; Kuzmin et al., 2003). Assuming thermal contraction and freeze–thaw cycles are the two processes that can explain the formation of patterned grounds, both processes affect only the uppermost meters of the ground because they are the consequence of

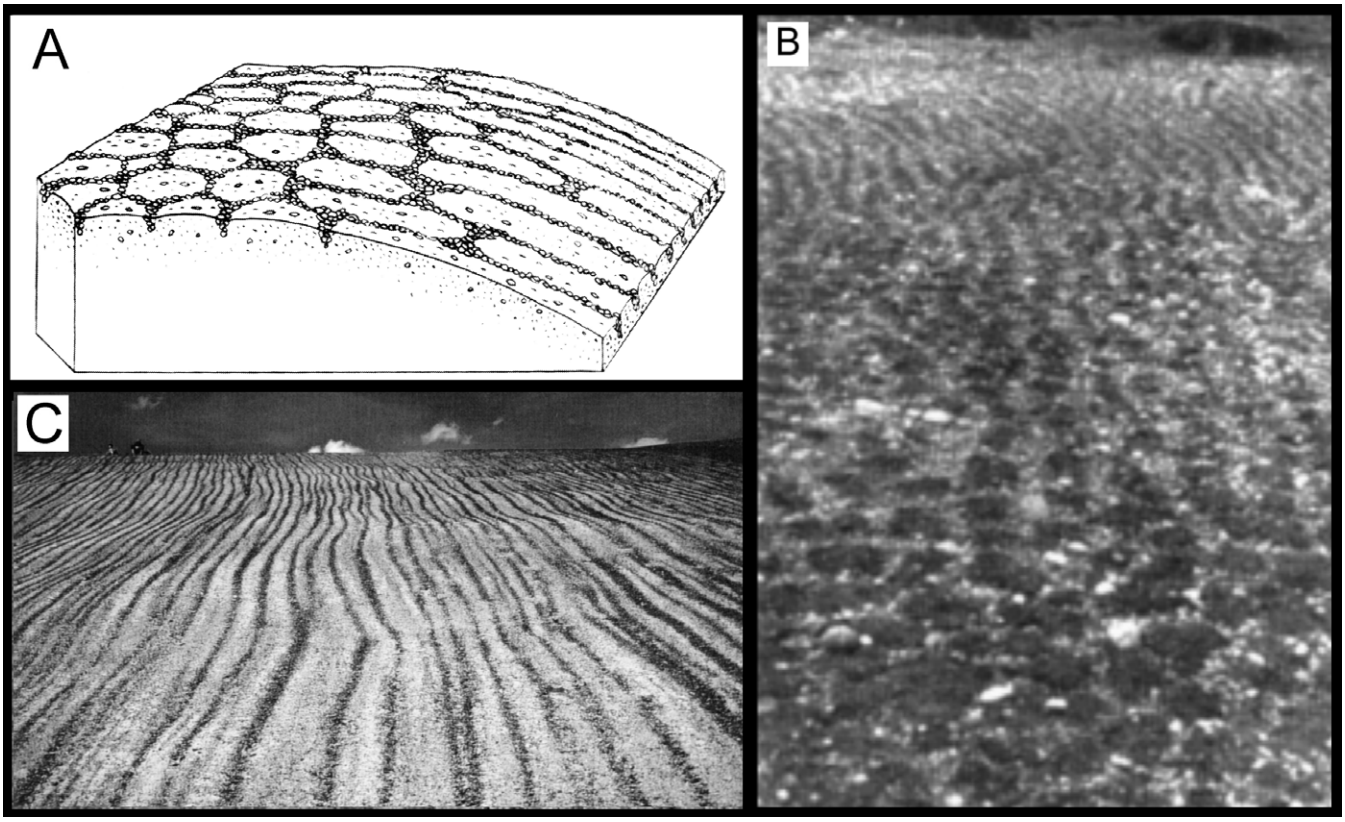

Fig. 6. (A) Sketch of sorted polygons which progressively transform into stripes (from Birkeland and Larson, 1989); (B) Small sorted polygons (30 cm wide) formed by diurnal freeze–thaw cycles which transform into stripes on a 3° steep slope in Northern Iceland (photo courtesy Dr. Ekkehard Schunke, University of Göttingen). (C) Slope stripes in Bolivia formed by diurnal cycles with spacing of about 40 cm (Photograph V. Jomelli, Institut de Géographie Physique, Meudon).

the propagation of seasonal or diurnal thermal waves. In the case of seasonal thaw, the layer which thaws each summer is on Earth typically about 1 m thick, possibly some tens of centimeters on Mars at past obliquity (Costard et al., 2002), whereas seasonal temperature changes can induce cracking down to a maximum of 2 or 3 m depending on the thermal properties of the ground (Mellon, 1997). These depths are equivalent to the maximum depth of hydrogen detected by the NS which is of about 1 m (Feldman et al., 2002). Ground ice deeper than 1 m may exist in regions equatorward of 55°–60° of latitudes without being detected by GRS but polygons may not exist at these latitudes because this ground ice is not reached by the seasonal thermal waves.

No relation between high latitude patterned grounds and albedo seems exist on the contrary of the Utopia large polygons which are more developed in regions of low albedo (Kuzmin et al., 2002; Yoshikawa, 2002). Most polygons remain unchanged even though they cross different geomorphic units on a given MOC image but the geometry of polygons is occasionally disturbed by differences of surface properties. Several images show dunes crossed by cracks (for example MOC #M11-00999, 79° S) whereas other images show dunes surrounded by cracks without being crossed (for example MOC #M08-02047). When cracks cross dunes they often display a geometry different than that on the surrounding plains, showing that different materials may play a role in the geometry of cracks. Another example shows ejectas of craters that are covered by small polygons whereas the surrounding terrain are crossed by larger polygons (for example MOC #M08-03306).

2.6. Stratigraphy and age of patterned grounds

With the exception of the LPC polygons type found around the south polar cap, polygons or stripes are poorly connected to geological units mapped using Viking images. They are found in the youthful deposits of martian high latitudes which are likely composed of dusty, loess like materials, containing interstitial water ice in large amounts (Tokar et al., 2002; Kreslavsky and Head, 2002; Feldman et al., 2002; Mischna et al., 2003; Head et al., 2003). A young age is confirmed by our study: among the 548 MOC images, only 15 craters between 20 and 150 m of diameter were observed. This number corresponds to fresh craters only, i.e., craters that are not affected by patterned ground. Of course, images have been selected using this criteria of youthfulness, but no terrains polewards of 60° exhibit strong densities of small impact craters. The determination of a maximum age is not relevant for large polygons which exist in small proportion but it is relevant for the S2 and S3 types which are the

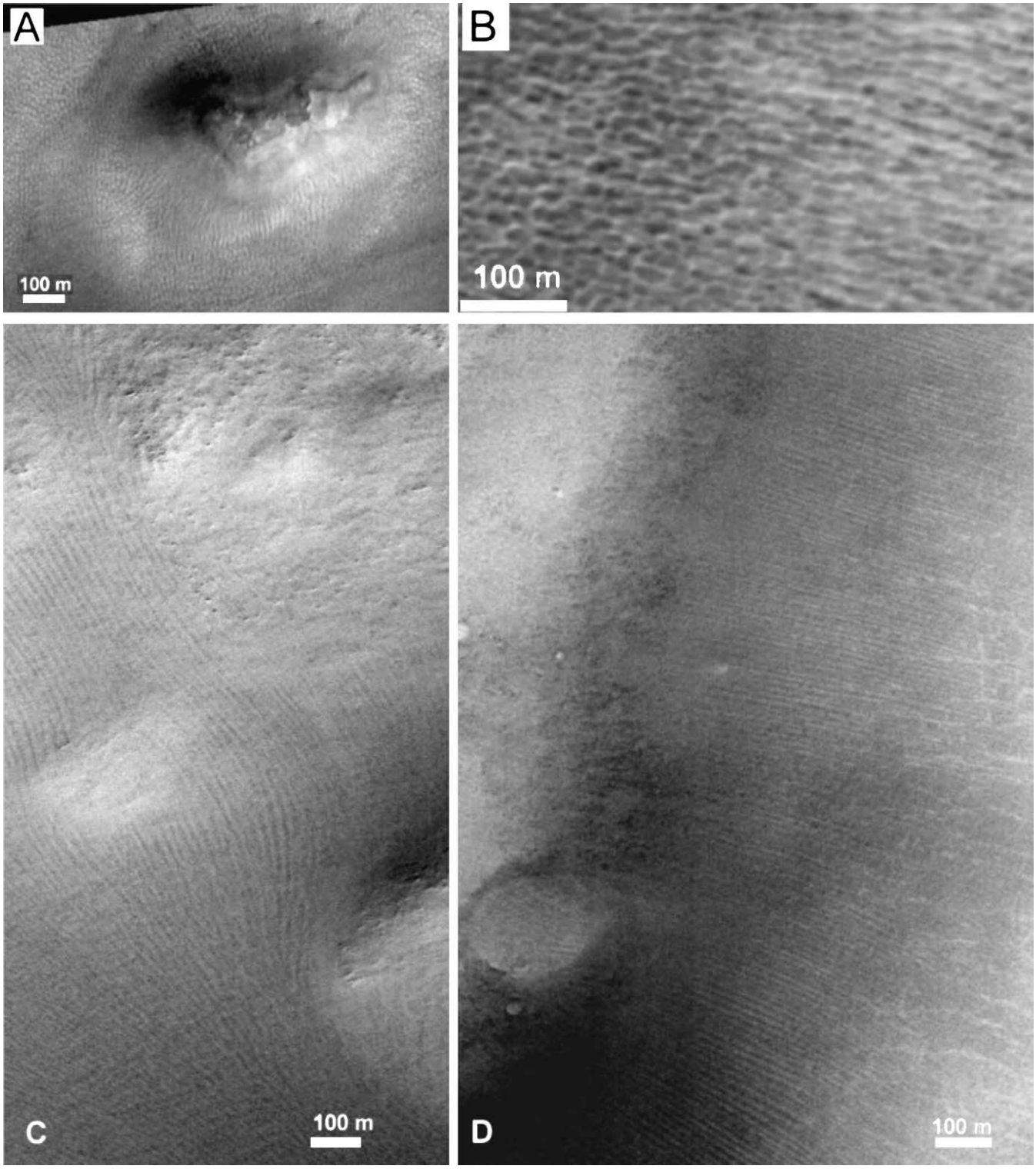

Fig. 7. (A) Small hill with stripes on flanks becoming small polygons on the plain. MOC image #M17-00992, 50.1° N, 24.6° W, $L_s = 27.4°$. (B) Small patterned ground S2 which transforms into stripes at the right of the image. MOC image #M03-01957, 64.6° S, 19.7° W, $L_s = 168.9°$. (C) MOC image #M02-02175, 64.9° S, 15.1° W, $L_s = 155.7°$, slope from top to bottom, light from below. (D) MOC image #E05-01306, 61.8° S, 29.9° W, $L_s = 178.2°$. Slope from left to right, light is from the left.

most abundant patterns. Assuming that they formed during the same period, the crater count gives a very young age of less than 1 Myr according to most recent models (Hartmann and Neukum, 2001).

It is possible that not all types of polygons are contemporary but the small number of craters does not permit to date them in relation to each other. Nevertheless, some chronological relations exist as the small S2 and S3 polygons over-

lay larger V and LT cracks in about 15 images. This shows that small polygons are younger than the larger V and LT polygons. On the other hand, several images of large crack networks, types V and LT (for example MOC image #M00-00602), show cracks eroded by the wind. This observation implies that they are not so young, or are not active anymore.

In summary, the first consequence of this classification is that there is not a single type of polygons and therefore probably not a single origin. The second consequence is that polygons are located in latitudes where ground ice is present at shallow depth of less than 1 m according to results from Mars Odyssey (Boynton et al., 2002; Feldman et al., 2002; Mitrofanov et al., 2003). So, many patterned grounds, if not all, are genetically related to this ground ice as predicted by previous studies (Mellon and Jakosky, 1995). The third consequence is that polygons are young, but not necessarily active at the present time. Mars is submitted to climatic cycles at the 10 to 100 kyr scale (e.g., Laskar and Robutel, 1993), so, if climatically controlled, they could be the result of temperature variations under past climates and not only current temperature variations.

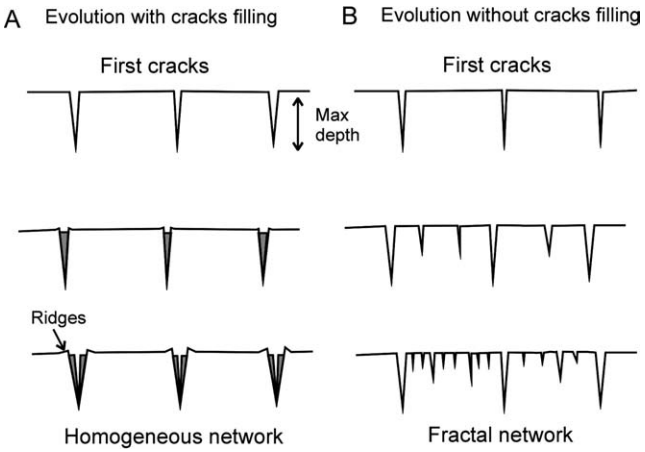

Fig. 8. Formation of cracks by thermal contraction. The complete evolution takes several hundred years if the cycle is annual. (A) The depth of cracks and the size of polygons depend on the thermal stress and ground properties. In presence of water or sand filling the cracks, cracks widen progressively without formation of smaller cracks. If the ground thaw seasonally, two symmetric pressure ridges form on each side of the cracks due to the volumetric expansion of water. (B) Without any filling of the cracks, cracks increase in width more slowly and smaller cracks form inside each polygons.

3. Origin of the different types of features observed

3.1. Theory of crack formation on the Earth and consequences for Mars

Many martian patterned grounds display bounding troughs indicating thermal contraction cracks. Thermal cracks in cold regions are formed by the contraction of the ground due to the propagation of the cold thermal wave during winter (e.g., French, 1996). Models show that the same effects can occur under martian temperatures (Mellon, 1997). Once formed, terrestrial cracks usually fill with surface meltwater and groundwater during summer. This water freezes in the fracture at the lower temperatures found in the subsurface. Because ice in fracture cavities is generally weaker than the frozen ground, fractures usually follow the same path from year to year (Plug and Werner, 2002). In this case, after the formation of polygons is completed, no new cracks form and the size of the polygons is fixed (Fig. 8A). This process also exists for sand filling the cracks and forming sand wedges (Murton et al., 2000; Sletten et al., 2003). This case is common in the arid regions where geomorphic effects due to wind are more efficient than those due to liquid water. Alternatively, the CO_2 frost cold trapped in cracks could play a similar role. However, CO_2 is not permanently condensed inside the cracks at current conditions (Kossacki and Markiewicz, 2002) like it should be for processes similar to ice wedges or sand wedges. Nevertheless, it is possible to imagine past colder conditions at different obliquities in which such a process was possible. On the other hand, in the absence of material filling the cracks, the tensile stress increases inside the newly formed polygons inducing new cracks with smaller sizes and smaller widths (Fig. 8B). Of course, intermediate cases can exist between these two end-members (Fig. 8).

Expansion of cracks of only 2 or 3 cm/years are recorded from field data because of the low thermal expansion of frozen ground which is estimated at a maximum of 3×10^{-4} K^{-1} (MacKay, 1980). Nevertheless, cracks can progressively widen up to 5 m because the formation of ice wedge polygons thus requires the repetition of seasonal temperature cycles over 10^2 or 10^3 years (Ugolini et al., 1973; Plug and Werner, 2001). Processes involving sand wedges polygons are usually slower than ice wedges because they depend on the availability of sand to be stored in the cracks. Evolution over periods of as much as 10^5 years has been reported for sand wedges (Sletten et al., 2003).

The identification of homogeneous polygons similar to ice wedge polygons is therefore not an evidence for the identification of seasonal liquid water. Nevertheless, ice wedge polygons on Earth are frequently bordered by small symmetric ridges or shoulders (Figs. 2C, 8A). These ridges are several tens of centimeters high and a few meters large and usually come from the progressive cycles of volumetric contraction and dilatation due to summer thawing of the material inside the polygons (MacKay, 1980; French, 1996). Sand wedges in Antarctica can also display pressure ridges (Sletten et al., 2003). In this case, the authors propose that the thermal expansion of the ground ice in summer can be sufficient to explain the formation of ridges. Nevertheless, this hypothesis remains to be tested because the thermal expansion of ground ice would have much lower effects than volumetric dilatation due to the transition of water ice in liquid water.

The penetration depth of cracks in the ground controls the size of the polygons. Terrestrial polygons formed by seasonal thermal contraction are usually 10 to 40 m large (French, 1996), exceptionally up to 80 m as in Siberia (Kuzmin et al., 2002). Theoretically, the width of first-order polygons corresponds to about three times the maximum depth of propagation of first-order cracks (Parker, 1999). For example, on Earth, seasonal variations produce ice wedges of typically 5–6 m deep for polygons 15–20 m wide (Lachenbruch, 1962). The depth of penetration of the seasonal cold wave in winter reaches 3–5 m at maximum. Cracks propagate only slightly deeper into the ground. Because the seasonal thermal wave is of the same order of magnitude on Mars and on Earth, polygons formed by seasonal thermal cracking should exhibit the same size range on Mars (Mellon, 1997). Thus, polygons 200 m large are at least five times wider than expected for seasonal contraction.

This difference may be explained by the fact that the permafrost is colder on Mars. Indeed, the terrestrial permafrost is relatively warm and soft close to the melting point. At temperatures 60 K colder, the frozen ground is more brittle, creating propagation of cracks strongly deeper than the stress created by the thermal wave (Maloof et al., 2002). Numerical models suggest that cracks formed by cyclic thermal variations can propagate into a cold cemented ground three to twenty-five times the depth affected by the thermal stress (Maloof et al., 2002). This possibility on Mars can be tested using the critical viscosity (Maloof et al., 2002):

$$\eta = \frac{1}{\varpi}\frac{E}{1-\nu}, \tag{1}$$

where E is the elastic Young modulus, typically 10 GPa for a frozen ground, ν is the Poisson ratio which varies from 0.12, at temperatures of 250 K or lower, to 0.4 close to the melting point of ice (Tsytovich, 1975), and $\varpi = 2\pi/T$ is the frequency of the temporal cycle T. If the ground is less viscous than this value, then the fracture cannot propagate (Maloof et al., 2002).

The calculated critical viscosity is 10^{17} Pa s for a temporal cycle corresponding to one martian year and 5×10^{16} Pa s for one terrestrial year. This value can be compared to the viscosity of the frozen ground known from mechanical experiments. Ice deforms by viscous creep according to a power-law relation (e.g., Duval et al., 1983) and ice-rock mixtures in a volume proportion of 1:1 are about 10 times more viscous than pure ice (Durham et al., 1992; Mangold et al., 2002b). At the stress produced by thermal contraction of typically 2 MPa (Mellon, 1997; Maloof et al., 2002), the critical value of the viscosity 10^{17} Pa s corresponds to a deformation at temperatures of about 210 K. Cracks can therefore propagate deeper than the thermal wave at temperatures colder than 210 K, a condition that is achieved at latitudes of 50° or higher (e.g., Mellon and Jakosky, 1995). By comparison, the viscosity at a terrestrial temperature of 260 K would give 10^{14} Pa s, much lower than the critical viscosity.

In the case of an annual cycle, the seasonal wave of typically 4 m would lead to cracks as deep as 100 m at maximum applying results of Maloof et al. (2002). Such deeper penetration could explain the larger size of martian polygons because the width is directly proportional to the depth of cracks by a factor of three (Parker, 1999) leading to a maximum size of polygons to 300 m. In the case of diurnal changes of temperatures rather than seasonal variations, the depth of penetration of the thermal wave is restricted to a few centimeters (e.g., Tokano, 2003). Polygons as large of 100 m are unlikely to form under such small variations. However, a diurnal cycle can propagate cracks deeper than the thermal wave if the viscosity is larger than 1.6×10^{14} Pa s, a condition that is possible at all latitudes on Mars. The observation of polygons formed by diurnal thermal variations would nevertheless require (1) the ground ice to be present very close to the surface (<10 cm) because the thermal wave is very shallow and (2) the polygons to be situated at latitudes lower than 75° because diurnal variations would be non efficient above 75°.

This critical viscosity provides a simple tool to explain the larger size of martian polygons. Nevertheless, the depth to which cracks propagate strongly depends on the properties of the ground (Maloof et al., 2002) which are poorly constrained on Mars as well as on Earth. Realistic values of propagation may not exceed factors of two or three, in which case other parameters could be involved to explain the larger sizes of polygons. For example, the lower martian gravity reduces the lithostatic pressure which may play a role in increasing displacements on tectonic faulting (Schultz et al., 2004). Furthermore, high obliquity periods create colder winter temperatures and warmer summer temperatures in polar regions. At an obliquity of 40° the average daily temperature at summer solstice would be 15 °C compared to −20 °C at current obliquity. Such stronger temperature differences could have increased the thermal stress and therefore produced deeper thermal cracks. Thus, three effects can concur to explain the larger sizes of some of the martian polygons.

3.2. Formation of large polygons connected to topography (LT)

LT polygons observed in the same range of latitude in both hemispheres may be controlled by seasonal temperature variations. Among the total number of 40 images, 32 are associated with craters floors or flanks, 6 with flanks of isolated hills and 2 with flanks of ancient valleys. The slopes on which they exist are not steep, ranging typically from a few degrees to no more than 10°. Polygons connected to craters are well developed on the floor of these craters and not only on their flanks (Fig. 9). Their homogeneous geometry similar to ice wedge polygons (Fig. 2C) questions their formation by processes involving seasonal thaw in concert

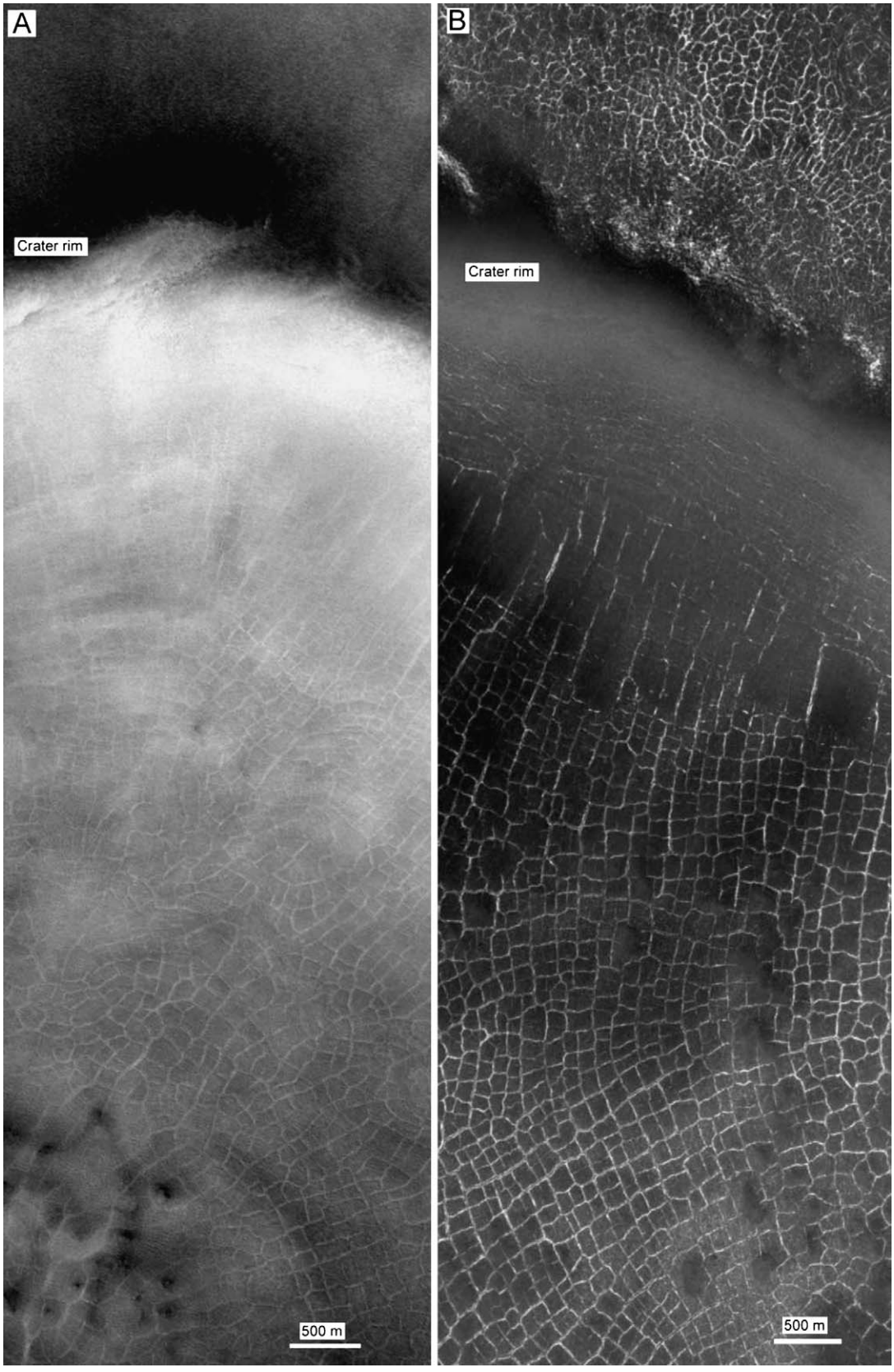

Fig. 9. (A) Half of a 20 km large crater in northern plains. Polygons with orthogonal cracks exist on the lower flank of the crater and random orthogonal cracks on the crater floor. Notice the small hills close to the center of the crater (at the bottom of the image) MOC image #E03-00299, 64.7° N, 292.9° S, $L_s = 140.6°$. (B) Half of a 15 km large crater in northern plains. Orthogonal polygons exist down to the central part of the crater. Notice smaller and randomly oriented polygons outside of the crater (top). MOC image #E1900409, 70.1° N, 295.3° W, $L_s = 601°$.

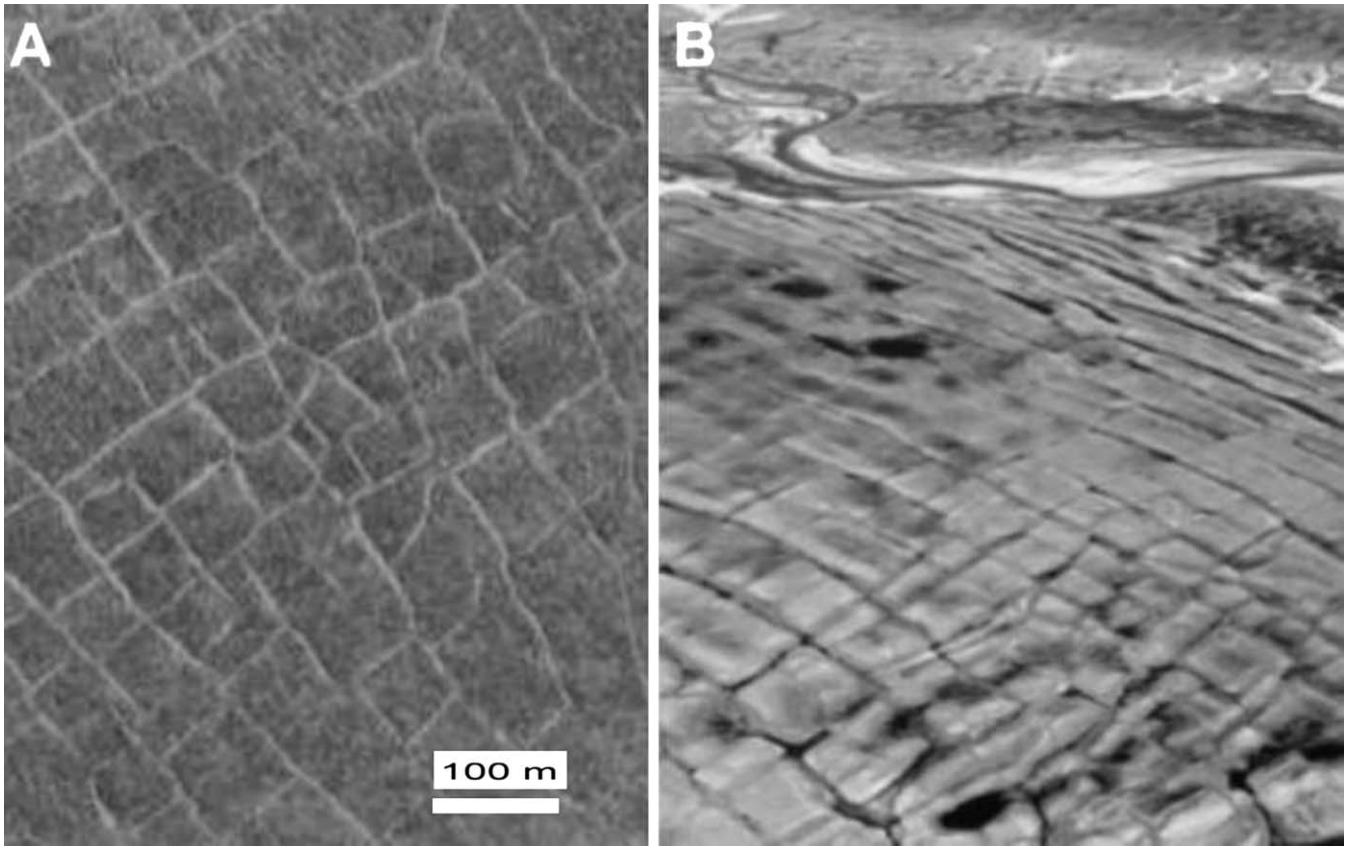

Fig. 10. (A) Rectangular cracks network on Mars. MOC image #M08-06179, 68° S, 310.4° W, $L_s = 231.4°$. (B) Rectangular network in Canada, NWT, GSC image #2002-329, 76° N, Prince Patrick Island.

with thermal contraction. Craters could be natural depressions for the retention of ground water. The involvement of standing bodies of water for some polygons inside such craters was previously proposed (Seibert and Kargel, 2001; Kuzmin et al., 2002) but only transient melting during summer season is required to form such polygons. The width of individual cracks of 5–10 m observed on LT polygons is similar to terrestrial examples caused by the cyclic widening of cracks (Fig. 8A). Nevertheless, whether this filling is due to water ice formed by frozen meltwater, to CO_2 ice, or to sand material deposed in the trough is difficult to discriminate. Craters also form natural sinks for sand because wind can provide fine materials to accumulate and fill cracks. Thus, a closer look to their geometry is needed to provide information about the context of their formation.

LT polygons are formed by oriented random orthogonal networks (class A) as well as orthogonal cracks (class B). On Earth, rectangular patterns (Fig. 10) form when the hydraulic head controls the initiation of cracks even if the slope is lower than 0.1° (French, 1996). On the other hand, MacKay (1995) shows terrestrial rectangular cracks which are perpendicular to slopes as steep as 30°. In this case, the rectangular network could be an indirect consequence of the main stress field on the slope. In both explanations, the orientation of cracks is systematically orthogonal and parallel to the slope, or concentric and parallel to the slope in the case of craters. Some observations could rely on the effect of the stress field due to the slope. For example, cracks often change from rectangular networks (class B) on the flank of craters to random orthogonal systems (class A) on the foot of these flanks (Fig. 9A). Nevertheless, some networks are still rectangular (class B) on the floor of craters where the effect of stress due to the slope is negligible (Fig. 9B). Moreover, this image shows that polygons outside the craters (top of Fig. 9B) are smaller and of different geometry which indicates that specific processes are involved on the bottom of the crater. Thus, if some orthogonal cracks are likely due to the stress field related to the crater flanks, others may indicate the role of transient meltwater.

Small hills can be seen in the center of some craters (left bottom of Fig. 9A). They could correspond to pingos formed during a wetter past (Soare and Peloquin, 2003). Pingos consist of broad and flat to small and narrow domes typically several tens or hundreds of meters large formed by doming of frozen ground due to freezing of injected water (MacKay, 1973, 1978; French and Dutkiewicz, 1976; French, 1996). Such features need warm summer temperatures in order to melt the ground ice at least partially on grain boundaries to create ground water flow in summer. Pingos often form in depressions associated with shallow transient lakes (French, 1996) making the presence of these hills on the floor of craters especially interesting.

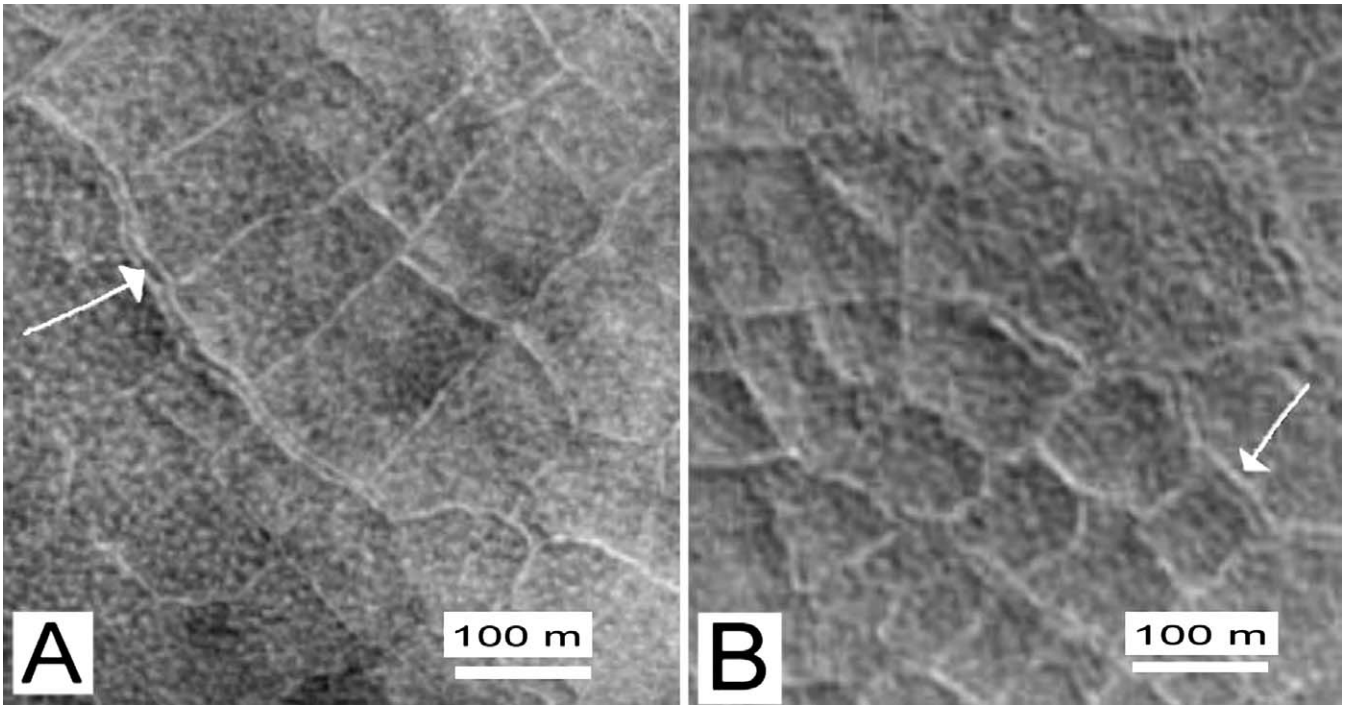

Fig. 11. Formation of ridges around cracks (similar as Fig. 2C on Earth) as indicated by the arrow in large polygons (100–200 m) on the floor of two different craters. Note the presence of hummocky pattern of S3 type about 10–15 m large over each ice-wedge like polygons similar to Fig. 2E on Earth. (A) MOC image #M00-00602, 65.7° N, 232° W, $L_s = 120.1°$. (B) MOC image #E03-00722, 61.2° N, 329.1° W, $L_s = 142.2°$.

Small ridges bounding polygons (Fig. 11) are similar to those formed by freeze–thaw cycles on Earth (Figs. 2C, 8A) favoring the role of groundwater in their formation (Baker, 2001) although dry processes may form similar patterns (Sletten et al., 2003). Small hummocks also cover the floor of the polygons (Fig. 11). They are 10–15 m large and specifically associated with LT polygons on 10 different images. They are classed as S3 type of patterned ground. Their association inside non-sorted polygons is strikingly analogous to that of mudboils over polygons on Earth (Fig. 2D). Mudboils, also named frost boils, have usually a limited extension of 1–3 m and are due to processes of frost heave in the active layer (e.g., French, 1996; Walker et al., 2003). Thus, the presence of these landforms could strengthen the hypothesis of seasonal thaw being an important factor in the formation of these polygons, although they could also be younger than the polygons having no genetic relations with them.

Finally, cyclic formation of sand wedges and orthogonal patterns due to stress fields on slopes may explain the geometry of some LT polygons but probably not all. Orthogonal crack networks on the floor of large craters together with the occurrence of ridges over cracks, potential frost boils and hills similar to pingos are an interesting combination which strongly suggests processes involving seasonal thaw acting in concert with thermal contraction. At current pressure and temperature conditions, liquid water on Mars is not stable long enough to fill the cracks, but past conditions may have permitted this process (Costard et al., 2002).

3.3. Formation of polygons around the south polar cap (LPC)

LPC polygons have a geometry similar to ice wedge polygons but bounding cracks are narrow without any bordering ridges and they are often longer than 1 km. There are also no rectangular polygons related to local slopes. These polygons likely formed by thermal contraction without involving seasonal thaw but their specific distribution around the south polar cap requires some additional explanations. CO_2 ice forms at cold temperatures of −125 °C close to the lowest temperatures on Mars. It has very slight temperatures variations during a martian year which should avoid any thermal cracking inside the permanent CO_2 cap itself. The images with LPC polygons therefore highlight locations with material rich in water ice rather than CO_2 ice. They can be used as indicator of water ice deposits in order to map the current front of the CO_2 cap similar to what was done with Themis thermal maps (Titus et al., 2003) and spectral data (Bibring et al., 2004). On Fig. 12, the front of the postulated residual CO_2 cap is recognizable by the circular pits of the swiss-cheese texture (Thomas et al., 2000; Malin et al., 2001). Some pristine cracks are also visible inside the swiss-cheese unit (Fig. 12B) which seem to correspond to the continuation of the LPC cracks inside the swiss-cheese terrains (Fig. 12). They could represent an effect of upward propagation of the cracks from underneath the cap into the CO_2 ice (Fig. 12C).

Images containing swiss-cheese terrains occasionally show polygons (Fig. 13) that were not mapped in the global

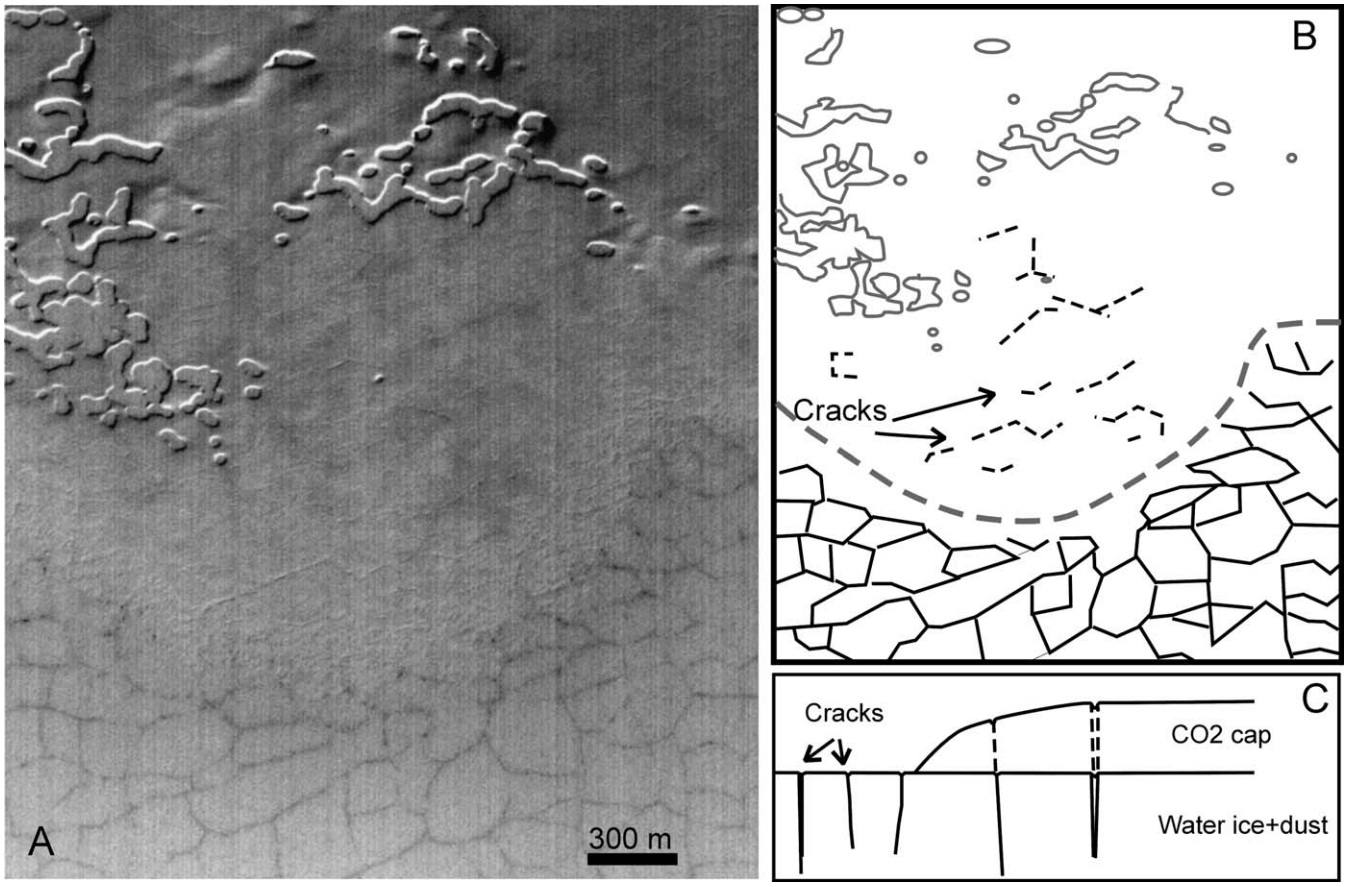

Fig. 12. (A) MOC image #M09-03178, 84.7° S, 55° W, $L_s = 243.3°$. Front of the south polar cap with swiss cheese features. (B) Schematic map of the MOC image. The front of the cap is the dotted gray line. Cracks in dotted lines are inside the swiss-cheese terrains. (C) Schematic cross section of the possible propagation of the cracks inside CO_2 ice to explain their presence at the surface of the CO_2 cap.

distribution of polygons because they should be associated with processes inside the CO_2 ice cap like the collapse of material due to the formation of swiss cheese depressions (Thomas, 2003). However, fractures formed around circular collapse zones have usually a specific geometry formed by the stress pattern around that zone (Fig. 13B). However, most cracks over the swiss cheese terrains shows a geometry similar to the random orthogonal network (class A) and sometimes hexagonal network (class C). Their average size of 100–300 m is also similar to the size of the LPC polygons outside the swiss cheese terrains. Thus, an alternative hypothesis for the formation of polygonal cracks over swiss cheese terrains is that they are due to the propagation of cracks formed by thermal contraction in the water ice rich terrains which underlie thin CO_2 deposits. Circular collapse may play a role in their shaping but the geometry seems not consistent with a pure collapse origin (Fig. 13C). This interpretation is consistent with the fact that the thickness of the CO_2 ice is probably very thin (<10 m) (Titus et al., 2003; Byrne and Ingersoll, 2003).

LPC polygons could be due to seasonal contraction but this would not explain they specific distribution and their occurrence underneath the CO_2 cap unaffected by the seasonal variations. The interpretation proposed hereafter states that they may be due to the long term thermal contraction created by the advance and retreat of the CO_2 residual cap. Indeed, the retreat of the CO_2 polar cap is currently observed by MOC images (Malin et al., 2001), implying that this cap was once larger. Thermal cracking occurs during the decrease of temperature. Thus, a surface blanketed by CO_2 is not heated anymore by the Sun and the surface temperature drops to the temperature of CO_2 around $-125\,°C$. A cold thermal wave would propagate even deeper as the duration of the blanketing is long (Fig. 14). After a period of advance of the CO_2 perennial cap, the residual cap would retreat and cracks would then become visible at the surface. This scenario may explain the occurrence of cracks underneath the CO_2 cap as proposed on Figs. 12 and 13. This scenario is also consistent with the lack of similar features around the northern cap because of the absence of CO_2 cap.

In such a scenario, the CO_2 cap would bury the water ice deposits during many years propagating a cold thermal wave deeper than the seasonal wave. In contrast to cyclic variations, a crack would not be able to propagate much deeper than the thermal wave like in the process described by Maloof et al. (2002) because it would be formed by only one strong episode. The depth D of the thermal wave can be approximated by the relation (e.g., Turcotte and Schubert,

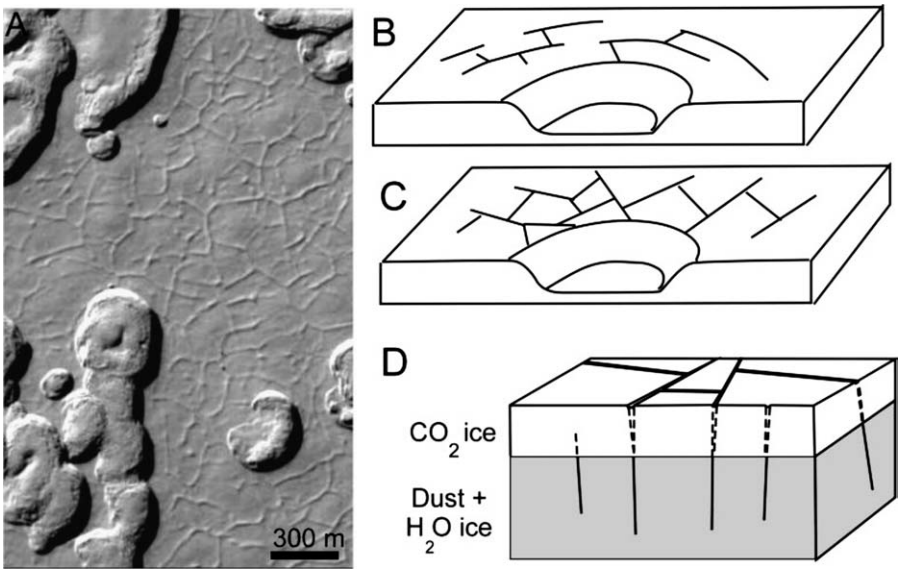

Fig. 13. (A) Cracks present over swiss cheese terrains MOC image #M08-00272, 86.1° S, 29.5° W, $L_s = 216.9°$. Cracks have same size (100–200 m) and geometry (class A cracks) than cracks in front of the swiss cheese terrains on Fig. 12. (B) Theoretical pattern of cracks due to collapse. (C) Theoretical pattern of cracks formed by thermal contraction without effect of collapse area. (D) Schematic 3D bloc of swiss cheese terrains over water ice rich polar deposits.

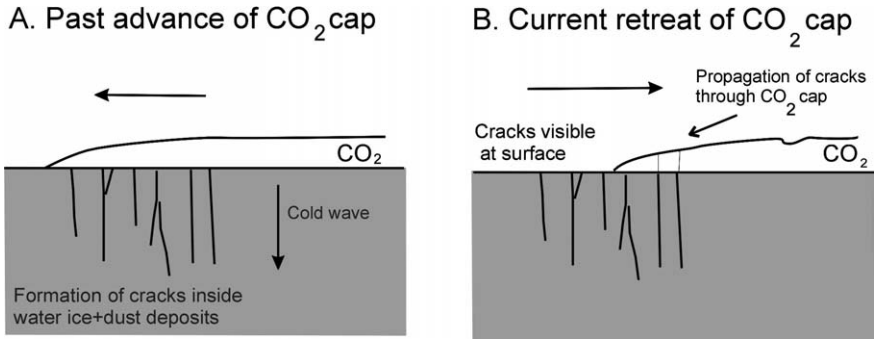

Fig. 14. Scenario of formation of polygons located around the south cap. (A) Past climate may have widened the CO_2 cap. The consequence is the propagation of a cold wave in the frozen ground which produce thermal contraction. (B) Geomorphic observations suggest the current retreat of the CO_2 cap (Malin et al., 2001). Cracks becomes visible at the surface and inside the swiss cheese terrains when crossed by cracks.

1982):

$$D = \sqrt{\frac{\kappa t}{\pi}}, \tag{2}$$

where t is the duration and κ the thermal diffusivity, fixed at 10^{-6} m^2/s (Johnston, 1981). The skin depth given by the relation correspond to $1/e$ the total depth of the wave penetration (Turcotte and Schubert, 1982). A depth of $D = 30$ m corresponds to a period of $t = 100$ terrestrial years. This depth is sufficient to produce polygons 100 m wide if we assume a factor of 3 in the width/depth ratio (Parker, 1999). Such duration of several hundreds of years is also consistent with timescales involved in the variations of the CO_2 cap (Malin et al., 2001; Byrne and Ingersoll, 2003). Thus, if this scenario is true, a better understanding of the geometry, distribution and formation of these LPC cracks could permit to reconstruct advances of the CO_2 cap over the last hundreds years.

3.4. Formation of polygons of heterogeneous sizes (V)

The fractal VF polygons fit the formation of cracks by cyclic variations but without material filling the cracks (Fig. 8B). The large width of some cracks (10 m) suggests a formation by cyclic variations such as thermal contraction, but no ridges surrounding cracks or other indicators of ground thawing are observed. VF polygons are dominant among the variable size polygons with 24 examples but the homogeneous geographic distribution of the three types suggests a similar origin. Volumetric contraction due to the desiccation of a muddy layer is unlikely because there is no association of cracks with topographic lows or with possible standing bodies of water and no preferred orientations is observed which would be due to tectonic stresses.

These polygons are located in regions poleward of 60° latitude where ground ice is detected by the Neutron Spectrometer confirming the potential role of thermal contraction

in their formation. However, if due to thermal contraction, the absence of similar features at the same latitudes in the northern hemisphere is enigmatic (Fig. 4). Does this mean that cracks observed in the southern hemisphere recorded unusual climate changes that did not occur in the northern hemisphere? In contrast to LPC polygons, they are probably not related to past advances of the CO_2 polar cap because they are typically located around 70° latitude which is too equatorial for such processes. Another explanation could come from their older age relative to the northern terrains. The surfaces of the northern hemisphere are more eroded or buried by younger deposits than surfaces of the southern hemisphere which appear older (Koutnik et al., 2002).

On the other hand, the northern hemisphere is not devoid of cracks because both S1 and LT types are observed. Different thermal conditions may have existed in the North in order to produce smaller or more homogeneous types of cracks. For example, the elevation difference of six kilometers between the northern and the southern hemisphere leads to a strong difference in atmospheric pressure. Elevation may also play a role in the thickness of the desiccated layer which overlays the ice rich layer (Maurice et al., 2004) and an asymmetry in the proportion of ground ice is observed on NS data with less ice being present in the southern regions (Feldman et al., 2003). These explanations are still speculative and, although the geometry of these large and variable polygons agrees with processes involving thermal contraction, more data are needed to understand their variability in geometry and their connection to climatic conditions.

3.5. Formation of homogeneous polygons smaller than 40 m (S)

S polygon types usually do not display cracks but their homogeneous shape could involve processes such as sorting of material by seasonal thaw. Small polygons such as those of Fig. 1B or stripes such as those of Fig. 7A are similar in shape to terrestrial sorted features (Figs. 2A, 6) but the size of sorted polygons on Earth are smaller from typically a few centimeters to several meters. A new model by Kessler and Werner (2003) explains sorted polygons by lateral squeezing of small stones because the freezing front progresses quicker downward in stones than in muddy soils. Such model explains sorted nets 1 to 5 m large formed by annual cycles but 20 m large sorted nets (Fig. 2B) remain unexplained. Such unusually large sorted nets are reported almost exclusively where thick continuous permafrost exists (Goldthwait, 1976), a situation that could be similar on Mars. On the other hand, the high latitudes terrain consists mainly of dust and ice deposits (Tokar et al., 2002; Mischna et al., 2003) in which sorting of material is uncertain. Features such as mud boils or hummocks due to frost heave in fine grained material should then be more frequent than sorted nets. “Frost heave” is the uplifting of the ground surface due to the formation of ice lens by percolation of unfrozen water between −10° and 0 °C (e.g., Konrad and Duquennoi, 1993). However, mud boils and hummocks are circular features typically 1 to 3 m large (e.g., Walker et al., 2003), thus also smaller than possible martian equivalents. Processes related to freeze–thaw cycles to explain small patterns remain therefore speculative especially due to the lack of evidence of sorting of material.

The S1 type displays cracks at a scale of 20–40 m which is similar to that found on Earth for polygons formed by thermal contraction (Lachenbruch, 1962) but this process alone cannot explain the formation of other small patterns S2 and S3. However, the sublimation of the ground ice is an additional process which is more important on Mars than on the Earth. It is suggested hereafter that small patterns could be the result of the degradation of contraction cracks by desiccation and erosion. The current atmospheric conditions imply that the ground at latitudes of 60°–70° is subjected to progressive desiccation in the top-most centimeters (Fanale et al., 1986; Mellon and Jakosky, 1995). This model assumes that the ground is a continuous medium. If the ground is fractured and contains cracks formed by thermal contraction, these fractures permit a more rapid sublimation of ice as it has been shown for fractures over glacier-like landforms (Fig. 6 of Mangold, 2003a). Ice grains in the fracture sublime quickly because they are in direct contact to the atmosphere. Solid grains then fall down into the trough, or are blown out by wind to the atmosphere, exposing the next ice grains to the atmosphere. Initial cracks would thus become wider and wider because of their progressive degradation (Figs. 15A–15C). That could explain why polygons are not separated by straight cracks but by more rounded bounding troughs. Despite it is difficult to imagine that S3 hummocks (Fig. 1D) were bounded by cracks before degradation, their connection to S2 type of polygons is shown on the histogram (Fig. 5A). At 50°–60°, the effect of sublimation is strong and plays a more important role in widening cracks than at 70°. The small patterned ground could thus be the poleward continuation of the dissected layers of the mid latitudes (Mustard et al., 2001) except that the process is efficient only in locations where cracks favor sublimation.

This hypothesis can be strengthened by comparing the ground ice distribution with thermal stress models. Temperature variations in an ice-free layer would not create cracks by thermal contraction. Neutron Spectrometer data shows that the ice table becomes shallower towards the poles (Feldman et al., 2002) (Fig. 15D). On the other hand, calculations by Mellon (1997) shows that all terrains poleward of 20°–30° could be affected by cracking if they contain ice in the uppermost meter. The critical stress reaches two or three meters at latitudes higher than 50°. Figure 15D compares the distribution of ground ice from NS data (gray) with the tensile stress found by Mellon (striped). This figure is very conceptual because both models, the ice-rich layer and the stress, are submitted to large uncertainties. Nevertheless, the combination of an ice-rich layer and a stress higher than the fracture boundary limits the development of possible cracks to regions poleward of 50°–55°,

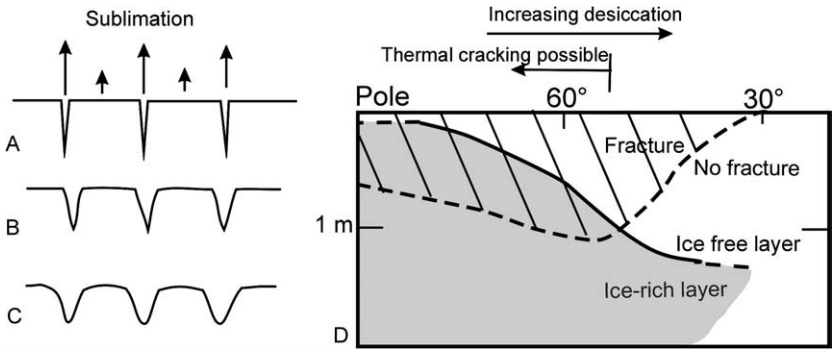

Fig. 15. (A) to (C) Progressive widening of cracks by sublimation of interstitial ice. (D) Theoretical comparison of thermal stress required to produce cracks and ice table deduced from GRS data. The region where thermal stress (striped, from Mellon, 1997) reaches the ice rich layer (gray) are located poleward of about 50°–55°. Desiccation increases to the equator, thus cracks are more degraded below 60° latitude. Thus, cracks at 70° of latitude would look like stage (A) of the degradation process at left whereas cracks at 50° of latitude would look like stage (C).

Table 2
Summary table of patterned ground types versus processes involved in their formation

Type	Thermal contraction	Ground thaw	Sublimation	CO_2 ice	Possible period of activity (past/current)
LT	Yes	Yes	Minor	?	Past high obliquity period
LPC	Yes	No	No	Yes	Last 100s years?
S1	Yes	No	Minor	?	Current climate (sublimation)
S2	Yes	Minor?	Yes	?	Current climate (sublimation)
S3	Yes	Minor?	Yes	?	Current climate (sublimation)
VF	Yes	Unlikely	Minor	?	Past climate?
VV	Yes	Unlikely	Minor	?	Past climate?
VCX	Yes	Unlikely	Minor	?	Past climate?
Hs	Possible	Yes	No	No	Past high obliquity period

Thermal contraction is the dominant process at all epochs. Sublimation is supposed to have developed recently and freeze–thaw cycles would have play a role during past high obliquity periods. Large uncertainties exist especially about the role of seasonal CO_2 frost in these processes. See caption of Table 1 for type description.

thus to regions where polygons are observed. Terrestrial studies highlight the geomorphic effect of the process of sublimation (Law and van Dijk, 1994), especially in cold and dry regions such as in Antarctica (Ugolini et al., 1973; Marchant et al., 2002; Sletten et al., 2003). A similar process of sublimation patterns is observed in subglacial till where pure ice layers exist underneath rocks (Marchant et al., 2002; Head et al., 2003). The slight difference between the process involved in Antarctica and the process proposed here is that the underlying layers on Fig. 16 are not necessarily pure ice but any frozen ground.

A question concerning the involvement of seasonal thermal contraction in the formation of different types of polygons S, L, and V is their difference in size from one type to another. Why are S polygons smaller than the L type if they are related to the same process of seasonal contraction? Assuming that they formed at the same period, small polygons could be due to thermal contraction by diurnal cycles, but this possibility is unlikely because the action of diurnal cycles takes place in the uppermost centimeters only which is ice free (Mellon and Jakosky, 1993; Feldman et al., 2003). Polygons could also be formed by seasonal thermal contraction but at different periods, such as higher obliquity periods during which polar regions are submitted to larger temperature variations. Martian polygons offer a wide range of variety which are far away to give all their secrets of formation.

4. Discussion: freeze–thaw cycles or no freeze–thaw cycles?

Thermal contraction represents the main mechanism able to form polygons at the surface of Mars (Table 2). Nevertheless, a few landforms may involve freeze–thaw cycles: (1) the large homogeneous polygons on crater floors (Figs. 9, 10, 11), (2) some of the small polygons with very homogeneous patterns (Fig. 1B) and polygons associated with stripes (Figs. 7A, 7B), and (3) striated soils Hs on hillslopes (Figs. 7C, 7D). For example, slope stripes not related to polygons are difficult to explain by other processes than seasonal thaw (Figs. 7C, 7D). The fact that the same width is found on different images favors a process similar to terrestrial processes despite the larger size than on Earth. Moreover, rocky material likely exists on slopes making sorting of grains easier to explain on slopes than on smooth plains mantled by dust.

Features indicative of seasonal thaw such as pingos would be difficult to distinguish from other features especially if martian pingos are similar to broad based pingos found in

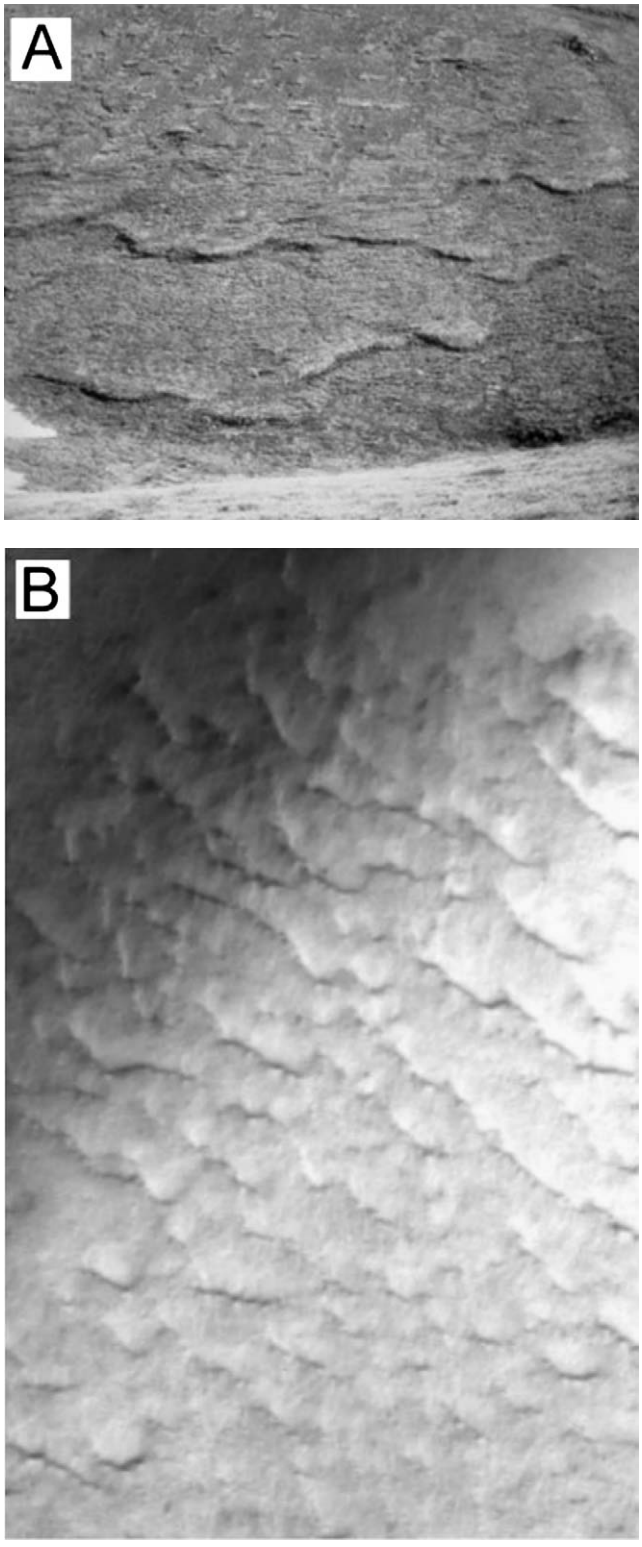

Fig. 16. (A) Solifluction lobes in Alaska, Suslositna Creek, about 1 m thick and tens of meters long (photograph NOAA National Geophysical Data Center). (B) One martian hillslope with lobes similar to solifluction lobes. The length of each lobe is of several hundreds of meters for a spacing of less than 100 m, so 2 or 3 times more than the terrestrial analog. The thickness of each lobe at the image resolution (4.1 m/pixel) is of the order of 1 m. Light is from the right, North is to the bottom. MOC image #M03-06278 (73.4° S, 314.5° W, $L_s = 180.8°$).

northern Alaska which are typically only 5 m high for 250 m large (Walker et al., 1985). Such pingos may exist on MOC images (Mangold, 2003b, Fig. 2) but circular features of less than 300 m in diameter are difficult to discriminate from other landforms such as buried craters. Pingos may nevertheless exist in connection to some ice wedge like polygons (Fig. 9). In addition, solifluction lobes are other possible landforms related to the periodic thaw of ground ice on periglacial hillslopes (Fig. 16A). Solifluction lobes are due to the creep of material at the surface because of the reduced frictional strength induced by porous water during summer (Harris et al., 1993). Solifluction is limited to the active layer, which is usually in the order of 1 m thick on Earth. Some MOC images show the presence of lobes very similar to terrestrial solifluction lobes (Fig. 16B). Their length of few hundred meters and potential thickness of a few meters is consistent with this hypothesis. The slope measured from MOLA data is 9° which is in the range of slopes of 3° to 15° at which solifluction is observed on the Earth (French, 1996). These lobes are restricted to the hillslope and are therefore difficult to explain by other processes such as aeolian ripples.

Necessary conditions for the formation of such features would be a significant soil moisture content and cyclic freezing and thawing of sufficient duration (French, 1996). Significant moisture means that at least a few percents of liquid water at grains boundaries are present to trigger hydraulic movements inside the ground. Current climatic conditions do not permit seasonal thaw at any latitudes. Nevertheless, orbital parameters such as eccentricity and obliquity controls insulation and climate at the surface of Mars (e.g., Laskar and Robutel, 1993). Recent periods were likely dominated by variations of obliquity which can vary from 10° to 45° in the last 10 myr (Mustard et al., 2001; Laskar et al., 2002; Costard et al., 2002; Head et al., 2003). Recent climate changes are involved in order to explain the formation of gullies (Costard et al., 2002). In that case, obliquity changes predicted by astronomical calculations (Laskar et al., 2002) can allow average daily temperatures above freezing at the latitudes considered (Mangold et al., 2002a).

Calculations of the surface temperature on Mars were performed for various latitudes and obliquities in order to investigate if such conditions could exist in the region of patterned grounds. The model used is the Global Climate Model (GCM) developed by the Laboratoire de Météorologie (LMD) (Forget et al., 1999). This model has been extensively validated through comparisons with available spacecraft observations, including in situ surface temperatures measurements (Lewis et al., 1999). According to these calculations (see Costard et al., 2002, for details), the daily average temperature reached values above the melting point of water on a flat surface around summer solstice at an obliquity of 40° (Fig. 17). An obliquity of 40° is possible in the last million years (Laskar et al., 2002; Head et al., 2003). Obliquity of 35° that occurred less than one half million years ago may have been enough to trigger seasonal thaw in certain conditions. These ages may be consistent with the

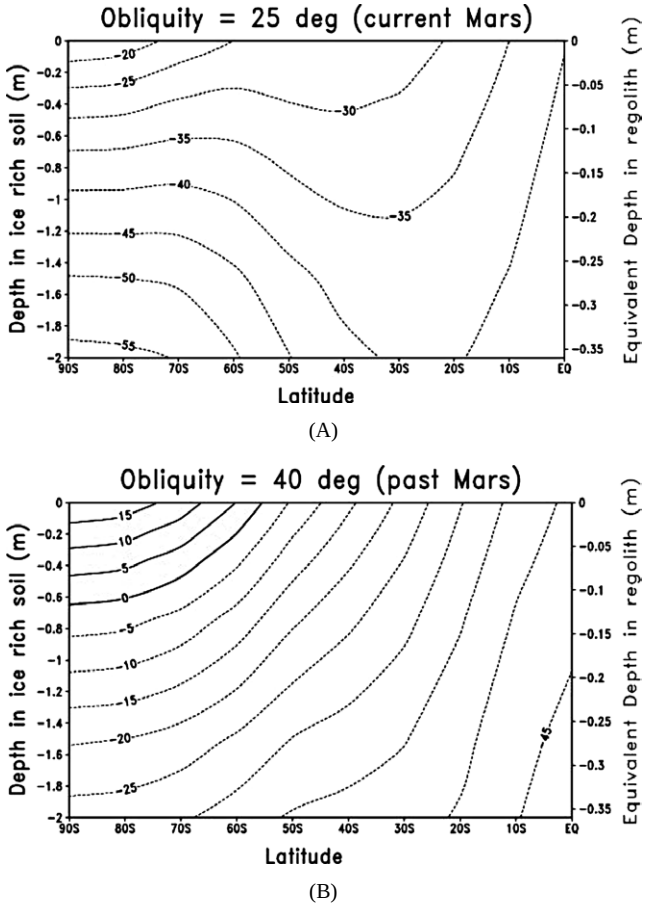

Fig. 17. Average daily temperature of the ground at two different obliquities. (A) Current obliquity does not permit above 0 °C temperatures of subsurface. (B) Obliquity of 40° allows near surface melting at latitudes poleward of 55°. Assuming an ice rich soil, depths of several tens of centimeters would be affected by this seasonal thaw. Graphs calculated from the Global Circulation Model of Mars of the "Laboratoire de Météorologie Dynamique, Paris" (Forget et al., 1999).

age of the polygons even though crater statistics cannot provide a more detailed chronology. The formation of most S polygons could have affected the most recent layer deposition several tens of thousand years ago without involving freeze–thaw cycles whereas LT and V polygons and some of the Hs stripes could correspond to older landforms that are still visible at the surface.

The presence of a freeze–thaw cycle requires the surface layers ice content to be recharged as ice is continuously lost by the progressive desiccation of the ground. Nevertheless, seasonal thaw may have existed in specific microenvironments such as craters interiors or hillslopes. Recent models identified crater floors (Russell et al., 2003) or poleward facing slopes (Schorghofer and Aharonson, 2003) as specific locations for water ice stability and deposition of ice. If snow occurred (Christensen, 2003) it would have favored the recharge of the surface layer in water ice and subsequent annual freeze–thaw cycles. A recent model also proposes the liquid water in the ground to be stable enough time before being sublimated (Hecht, 2002) whereas the winter CO_2 frost may protect ground ice from sublimation before thawing (Costard et al., 2002).

The consequence of past seasonal thaw is important, not only for the formation of sorted polygons and similar features, but also for the subsequent processes of frost heave and ice segregation in the ground. When the ground is at temperatures between −10 °C and 0 °C, unfrozen water exists at the contact with grains (e.g., Dash et al., 1995). A large quantity of unfrozen water is present when solid grains are small like in clay or silt (e.g., Johnston, 1981). This amount increases exponentially up to the melting point (e.g., Johnston, 1981). With a progressive change in temperature this unfrozen water moves downward or upward producing what is called cryogenic suction (Konrad and Morgenstern, 1980; Konrad and Duquennoi, 1993). The unfrozen water then freezes at one point in the soil column creating ice lenses at all scales from several μm to several meters thick (e.g., French, 1996). This process can produce supersaturated layers in the uppermost meters of the ground that are filled by 60 to 80% in volume of interstitial ice (Pollard and French, 1980; Cheng, 1983). Now, the Gamma Ray Spectrometer shows the presence of an ice-rich layers with unexplained proportion of more than 60% of ice in volume (Boynton et al., 2002; Feldman et al., 2002). Cycles of frost deposits layered with dust (Mischna et al., 2003) are a possible explanation of the large amount of interstitial ice but past periods with seasonal thaw and segregation of ice are an alternative solution.

Older periods of obliquity higher than 40°–60° are predicted several millions or tens of million of years ago (Laskar and Robutel, 1993). Such periods could have lead to the more developed action of cyclic thawing in the summer season. Features corresponding to such periods should be found on MOC images but the rapid mantling of polar regions may hide landforms such as polygons. Nevertheless, the strong degradation of craters 1–5 km diameter at 60°–70° latitude into very shallow topography, named "pathological craters," could highlight effects of transient episodes of surface melting by filling craters more efficiently than any eolian processes (Hartmann and Esquerdo, 1999). Ice wedges like polygons observed in Utopia Planitia at mid latitudes could also indicate such older periods (Seibert and Kargel, 2001) but the lack of similar polygons at the same latitudes in other regions of the planet prevent possible interpretations of these polygons as related to climatic effects. On the other hand, the episodic occurrence of freeze–thaw cycles throughout the last tens or hundreds of million years would have played a major role in reshaping the topography of polar regions and it could be a major factor in the smoothing of high latitude regions at the MOLA scale (Kreslavsky and Head, 2003b). Finally, new interpretations of spectral data from TES (Thermal Emission Spectrometer) suggest that altered basaltic surfaces in regions of high latitudes could be due to the progressive alteration of the ground by cyclic climatic variations (Wyatt et al., 2003). Transient liquid water in the ground would certainly have a strong effect

on ground alteration by increasing the kinetics of weathering.

5. Conclusions and implications for future missions

A classification of patterned grounds on Mars was done using the MOC image datasets M01 to E06. This study shows that they can be interpreted by different processes depending on their geometry and distribution:

1. Patterned grounds have been classed in ten types including polygons, hummocks and stripes. Their distribution above 55° latitudes correlates with the distribution of ground ice found by the Neutron Spectrometer onboard Mars Odyssey.

2. At least 5 types of patterned grounds are controlled by the climate because they are located at the same latitudes between 55° and 75° in both hemispheres. Comparisons with Earth analogues show that they are likely produced by processes due to seasonal temperature variations such as thermal contraction and seasonal thaw.

3. Polygons on Mars are often larger than on Earth by a factor of up to five. This effect can be due to deeper propagation of cracks because of the colder temperatures of martian permafrost. Large cracks can also be due to larger temperatures variations in past periods.

4. Homogeneous polygons 50 to 200 m wide found in the interiors of craters or at the foot of hillslopes are often similar to ice wedge polygons on Earth formed by a combination of thermal contraction and seasonal thaw.

5. Heterogeneous networks of large cracks with variable sizes exist mainly at the high latitudes of the southern hemisphere. They probably formed by thermal contraction but their complex geometry is still enigmatic.

6. Large (50–300 m) homogeneous polygons bounded by straight and narrow cracks are found around the south polar cap. These cracks developed in ice rich deposits which exists underneath the residual CO_2 cap. The formation of these cracks could be the result of the blanketing by the CO_2 cap and subsequent contraction of the water ice deposits.

7. Small polygons and hummocks (15–40 m) are dominant in number. Cracks are not observed directly except for a small distinct class of polygons but thermal contraction and widening by the desiccation of the surface layer may explain their formation.

8. Several features such as some small patterns, large homogeneous polygons on crater floor, slopes stripes or solifluction lobes could correspond to features formed by processes involving freeze–thaw cycles during past episodes of high obliquity (35° or more). Such past episodes of freeze–thaw cycles may have been enhanced in specific environments such as crater interiors or hillslopes.

9. All types of patterned grounds observed on Mars are recent (<10 Myr) but they did not form simultaneously. The most recent ones are likely the abundant small patterns and the cracks around the south polar cap (Table 2). Large homogeneous polygons and hillslopes stripes could have recorded periods during which seasonal temperatures variations were higher than at the present time.

Cyclic ground thaw in summer periods during past high obliquity is possible for several examples detailed in this study but this hypothesis still needs to be confirmed. Future high resolution images of the HiRise instrument onboard the Mars Reconnaissance Obiter mission (McEwen et al., 2003) could improve these interpretations by having more detailed observations of the size, spacing, rock sorting and geometry of these landforms. If high latitude terrains were submitted to cyclic periods with seasonal thaw, this process would be fundamental for exobiological researches (McKay, 2003), because life is able to survive in environments of permanently cold regions on Earth where only episodic warm periods exist (Friedmann, 1994). The Phoenix lander (2007) will explore these regions of high latitudes in order to find ground ice and indications of present or past life (Smith, 2003). The identification of specific locations such as crater interiors in which atmospheric conditions may have favored the transient apparition of water in the ground in the past is important in the selection of landing sites for such mission.

Acknowledgments

The author acknowledges the use of Mars Orbiter Camera images processed by Malin Space Science Systems that are available at http://www.msss.com/moc_gallery/ and at the USGS at http://ida.wr.usgs.gov/ and the Canadian Geological Survey at http://sts.gsc.nrcan.gc.ca. The author thanks F. Costard, F. Forget, V. Jomelli, J. Lanz, and J.-P. Peulvast for helpful discussions. This work is granted by the Programme National de Planétologie (PNP) of the Institut National des Sciences de l'Univers (INSU), France, and by the European network MAGE (Mars Geophysical network).

References

Baker, V.R., 2001. Water and the martian landscape. Nature 412 (6843), 228–236.

Ballantyne, C.K., 1996. Formation of miniature sorted patterns by shallow ground freezing: a field experiment. Permafrost Periglac. 7, 409–424.

Bibring, J.-P., Langevin, Y., Poulet, F., Gendrin, A., Gondet, B., Berthé, M., Soufflot, A., Drossart, P., Combes, M., Belluci, G., Moroz, V., Mangold, N., Schmitt, B., the OMEGA Team, 2004. Perennial water ice identified around the Mars south pole. Nature 428, 627–630.

Birkeland, P.W., Larson, E.E., 1989. Putnam's Geology, fifth ed. Oxford Univ. Press, London.

Boynton, W.V., 26 colleagues, 2002. Distribution of hydrogen in the near-surface of Mars: evidence for subsurface ice deposits. Science 297 (5578), 81–85.

Byrne, S., Ingersoll, A.P., 2003. A sublimation model for martian south polar ice features. Science 299, 1051–1053.

Cabrol, N.A., Grin, E.A., 2002. The recent Mars global warming and/or south pole advance hypothesis: global geological evidence and reasons why gullies could still be forming today. Lunar Planet. Sci. 32. Abstract 1058.

Cheng, G., 1983. The mechanism of repeated—segregation for the formation of thick layered ground ice. Cold Reg. Sci. Technol. 8, 57–66.
Christensen, P.R., 2003. Formation of recent martian gullies through melting of extensive water-rich snow deposits. Nature 422, 45–48.
Costard, F., Forget, F., Mangold, N., Peulvast, J.-P., 2002. Formation of recent martian debris flows by melting of near-surface ground ice at high obliquity. Science 295, 110–113.
Dash, J.G., Haiying, F., Wettlaufer, J.S., 1995. The premelting of ice and its environmental consequences. Rep. Prog. Phys. 58, 115–167.
Durham, W.B., Kirby, S.H., Stern, L.A., 1992. Effects of dispersed particulates on the rheology of water ice at planetary conditions. J. Geophys. Res. 97, 20883–20897.
Duval, P., Ashby, M.F., Anderman, I., 1983. Rate controlling processes in the creep of polycrystalline ice. J. Phys. Chem. 87, 4066–4074.
Fanale, F.P., Salvail, J.R., Zent, A.R., Postawko, S.E., 1986. Global distribution and migration of subsurface ice on Mars. Icarus 67, 1–18.
Feldman, W.C., 12 colleagues, 2002. Global distribution of neutrons from Mars: results from Mars Odyssey. Science 297 (5578), 75–78.
Feldman, W.C., Prettyman, T.H., Maurice, S., Plaut, J.J., Bish, D.L., Vaniman, D.T., Mellon, M.T., Metzger, A.E., Squyres, S.W., Karunatillake, S., Boynton, W.V., Elphic, R.C., Funsten, H.O., Lawrence, D.J., Tokar, R.L., 2003. The global distribution of near-surface hydrogen on Mars. J. Geophys. Res. Planets. Submitted for publication.
Forget, F., Hourdin, F., Fournier, R., Hourdin, C., Talagrand, O., Collins, M., Lewis, S., Read, P.L., Huot, J.P., 1999. Improved general circulation models of the martian atmosphere from the surface to above 80 km. J. Geophys. Res. Planets 104 (E10), 24155–24175.
Fowler, A.C., Krantz, W.B., 1994. A generalized secondary frost heave model. SIAM J. Appl. Math. 54 (6), 1650–1675.
Francou, B., Le Méhauté, N., Jomelli, V., 2001. Factors controlling spacing distances of sorted stripes in a low latitude, Alpine environment (Cordillera Real, 16° S, Bolivia). Permafrost Periglac. 12, 367–377.
French, H.M., 1996. The Periglacial Environment, second ed. Longman, London.
French, H.M., Dutkiewicz, L., 1976. Pingos and pingo-like forms, Banks Island, Western Canadian Arctic. Biuletyn Peryglacjalny 26, 211–222.
Friedmann, E.I., 1994. Permafrost as microbial habitat. In: Gilichinsky, D.A. (Ed.), Viable Microorganisms in Permafrost. Russian Academy of Sciences, Pushchino, Russia, pp. 21–26.
Gleason, K.J., Krantz, W.B., Caine, N., George, J.H., Gunn, R., 1986. Geometrical aspects of sorted patterned ground in recurrently frozen soil. Science, 216–220.
Goldthwait, R.P., 1976. Frost sorted patterned ground. Quaternary Res. 6, 27–35.
Hallet, B., Prestrud, S., 1986. Dynamics of periglacial sorted circles in western Spitsbergen. Quaternary Res. 26, 81–99.
Harris, C., Gallop, M., Coutard, J.-P., 1993. Physical modelling of gelifluction and frost creep: some results of a large-scale laboratory experiment. Earth Surf. Proc. Land. 18, 383–398.
Hartmann, W.K., Esquerdo, G., 1999. Pathological martian craters: evidence for a transient obliteration event. Meteorit. Planet. Sci. 34, 159–165.
Hartmann, W.K., Neukum, G., 2001. Cratering chronology and evolution of Mars. Space Sci. Rev. 96 (1–4), 165–194.
Head, J.W., Mustard, J.F., Kreslavsky, M.A., Millike, R.E., Marchant, D.E., 2003. Recent ice ages on Mars. Nature 426, 797–802.
Hecht, M.H., 2002. Metastability of liquid water on Mars. Icarus, 373–386.
Hiesinger, H., Head, J.W., 2000. Characteristics and origin of polygonal terrain in southern Utopia Planitia, Mars. J. Geophys. Res. 105 (E5), 11999–12022.
Johnston, G.H., 1981. Permafrost: Engineering Design and Construction. Wiley, New York.
Kessler, M.A., Werner, B.T., 2003. Self-organization of sorted patterned ground. Science 299, 380–383.
Konrad, J.-M., Duquennoi, C., 1993. A model for water transport and ice lensing in freezing soils. Water Resour. Res. 29 (9), 3109–3124.
Konrad, J.-M., Morgenstern, N.R., 1980. The segregation potential of a freezing soil. Can. Geotech. J. 18, 482–491.
Kossacki, K.J., Markiewicz, W.J., 2002. Martian seasonal CO_2 ice in polygonal troughs in southern polar region: role of the distribution of subsurface H_2O ice. Icarus 160, 73–85.
Koutnik, M., Byrne, S., Murray, B., 2002. South polar layered deposits on Mars: the cratering record. J. Geophys. Res. 107 (E11), 10-1.
Krantz, W.B., 1990. Self-organization manifest as patterned ground in recurrently frozen soils. Earth Sci. Rev. 29, 117–130.
Kreslavsky, M.A., Head III, J.W., 2002. Mars: nature and evolution of young latitude dependent water-ice rich mantle. Geophys. Res. Lett. 29 (15), 14-1.
Kreslavsky, M.A., Head III, J.W., 2003a. North–south topographic slope asymmetry on Mars: evidence for insolation-related erosion at high obliquity. Geophys. Res. Lett. 30 (15), 1-1.
Kreslavsky, M.A., Head III, J.W., 2003b. Polar wander in the geological history of Mars: constraints from topography statistics. In: 3rd Mars Polar Conf., Lake Louise. Abstract 8085.
Kuzmin, R.O., Ershow, E.D., Komarow, I.A., Kozlov, A.H., Isaev, V.S., 2002. The comparative morphometric analysis of polygonal terrain on Mars and the Earth high latitude areas. Lunar Planet. Sci. 33. Abstract 2030.
Kuzmin, R.O., Mitrofanov, I.G., Litvak, M.L., Boynton, W.B., Saunders, R.S., 2003. Mars: detaching of the free water signature presence regions on the base of HEND/Odyssey data and their correlation with some permafrost features from MOC data. Lunar Planet. Sci. 34. Abstract 1369.
Lachenbruch, A., 1962. Mechanics of thermal contraction cracks and ice-wedge polygons in permafrost. Geol. Soc. Am., Spec. Paper 70. 69 p.
Lachenbruch, A., 1966. Contraction theory of ice wedge polygons; a qualitative discussion. In: Proc. 1st Int. Permafrost Conf. NRC Canada, Publ., vol. 1287, pp. 63–71.
Laskar, J., Robutel, P., 1993. The chaotic obliquity of the planets. Nature 361 (6413), 608–612.
Laskar, J., Levrard, B., Mustard, J.F., 2002. Orbital forcing of the martian polar layered deposits. Nature 419, 375–378.
Law, J., van Dijk, D., 1994. Sublimation as a geomorphic process: a review. Permafrost Periglac. 5, 237–249.
Leverington, D.W., 2003. Preliminary results from a survey of candidate permafrost and periglacial features on Mars. In: 3rd Mars Polar Conf., Lake Louise. Abstract 8013.
Lewis, S.R., Collins, M., Read, P.L., Forget, F., Hourdin, F., Hourdin, C., Talagrand, O., Huot, J.-P., 1999. A climate database for Mars. J. Geophys. Res. Planets 104 (E10), 24177–24194.
Lucchitta, B.K., 1983. Permafrost on Mars: polygonally fractured ground. In: Permafrost, 4th Int. Conf. Proceedings. National Academy Press, Washington, pp. 744–749.
McEwen, A.S., the HiRise Team, 2003. MRO's high resolution imaging science experiment (HiRISE): science expectations. In: 6th Int. Mars Conf. Pasadena. Abstract 3217.
MacKay, J.R., 1973. The growth of pingos, Western Arctic Coast, Canada. Can. J. Earth Sci. 10, 979–1004.
MacKay, J.R., 1978. Sub-pingo water lenses, Tuktoyaktuk Peninsula, Northwest Territories. Can. J. Earth Sci. 8, 1219–1227.
MacKay, J.R., 1980. The deformation of ice-wedge polygons, Garry Island, Northwest Territories. Geol. Surv. Canada 80A (1A), 287–291.
MacKay, J.R., 1995. Ice wedges on hillslopes and landform evolution in the late quaternary, western Arctic coast, Canada. Can. J. Earth Sci. 32 (8), 1093–1105.
McKay, C.P., 2003. The polar regions of Mars and the search for evidence of life on Mars. In: 3rd Mars Polar Conf., Lake Louise. Abstract 8051.
Maloof, A.C., Kellog, J.B., Anders, A.M., 2002. Neoproterozoic sand wedges: crack formation in frozen soils under diurnal forcing during a snow ball Earth. Earth Planet. Sci. Let. 204, 1–15.
Malin, M.C., Edgett, K.S., 2000. Evidence for recent groundwater seepage and surface run-off on Mars. Science 288, 2330–2335.
Malin, M.C., Edgett, K.S., 2001. Mars Global Surveyor Mars Observer Camera: interplanetary cruise through primary mission. J. Geophys. Res. 106 (E6), 23429–23571.

Malin, M.C., Caplinger, M.A., Davis, S.D., 2001. Observational evidence for an active surface reservoir of solid carbon dioxide on Mars. Science 294, 2146–2148.

Mangold, N., 2003a. Geomorphic analysis of lobate debris aprons on Mars at MOC scale: evidence for ice sublimation initiated by fractures. J. Geophys. Res. Planets 108 (E4), 2-1.

Mangold, N., 2003b. Patterned ground on Mars: evidence for recent freeze–thaw cycles in high latitudes. In: Proc. 8th Int. Permafrost Conf., Zurich, pp. 723–728.

Mangold, N., Costard, F., Forget, F., Peulvast, J.P., 2002a. High latitude patterned grounds on Mars: evidence for recent melting of near-surface ground ice. Lunar Planet. Sci. 33. Abstract 1219.

Mangold, N., Allemand, P., Duval, P., Géraud, Y., Thomas, P., 2002b. Experimental and theoretical deformation of ice–rock mixtures: implications on rheology and ice content of martian permafrost. Planet. Space Sci. 50, 385–401.

Mangold, N., Maurice, S., Feldman, W.C., Costard, F., Forget, F., 2003. Geographical relationships between small scale polygons and ground ice distribution from Neutron Spectrometer on Mars. In: 3rd Mars Polar Conf., Lake Louise. Abstract 8043.

Mangold, N., Maurice, S., Feldman, W.C., Costard, F., Forget, F., 2004. Spatial relationships between patterned ground and ground ice detected by the Neutron Spectrometer on Mars. J. Geophys. Res. Planets. In press.

Marchant, D.R., Lewis, A., Phillips, W.C., Moore, E.J., Souchez, R.A., Denton, G.H., Sugden, D.E., Potter Jr., N., Landis, G.P., 2002. Formation of patterned-ground and sublimation till over Miocene glacier ice in Beacon Valley, Antarctica. Geol. Soc. Am. Bull. 114 (6), 718–730.

Masson, P., Carr, M.H., Costard, F., Greeley, R., Hauber, E., Jaumann, R., 2001. Geomorphologic evidence for liquid water on Mars. Space Sci. Rev. 96, 333–364.

Maurice, S., Gasnault, O., Feldman, W.C., Prettyman, T.H., Elphic, R.C., Laurence, D.J., 2004. Burial depth of the reservoir of hydrogen at equatorial latitude on Mars. Lunar Planet. Sci. 35. Abstract 1866.

Mellon, M.T., 1997. Small-scale polygonal features on Mars: seasonal thermal contraction cracks in permafrost. J. Geophys. Res. 102 (E11), 25617–25628.

Mellon, M.T., Jakosky, B.M., 1993. Geographic variations in the thermal and diffusive stability of ground ice on Mars. J. Geophys. Res. Planets 98 (E2), 3345–3364.

Mellon, M.T., Jakosky, B.M., 1995. The distribution and behavior of martian ground ice during past and present epochs. J. Geophys. Res 100, 11781–11789.

Mischna, M.A., Richardson, M.I., Wilson, R.J., Mac Cleese, D.J., 2003. On the orbital forcing of martian water and CO_2 cycles: a general circulation model study with simplified volatile schemes. J. Geophys. Res. 108 (E6), 16-1.

Milliken, R.E., Mustard, J.F., Goldsby, D.L., 2003. Viscous flow features on the surface of Mars: observations from high-resolution Mars Orbiter Camera (MOC) images. J. Geophys. Res. 108 (E6), 11-1. Art. No. 5057.

Mitrofanov, I.D., the HEND Team, 2003. Maps of subsurface hydrogen from the high-energy neutron detector, Mars Odyssey. Science 287, 78–81.

Murton, J.B., Worsley, P., Gozdzik, J., 2000. Sand veins and wedges in cold aeolian environments. Quaternary Sci. Rev. 19, 899–922.

Mustard, J.F., Cooper, C.D., Rifkin, M.K., 2001. Evidence for recent climate change on Mars from the identification of youthful near-surface ground ice. Nature 412, 411–413.

Parker, A.P., 1999. Stability of arrays of multiple edge cracks. Eng. Fract. Mech. 62, 577–591.

Pechmann, J.C., 1980. The origin of polygonal troughs on the martian northern plains. Icarus 42, 185–210.

Peterson, R.A., Krantz, W.B., 2003. A mechanism for differential frost heave and its implications for patterned ground formation. J. Glaciol. In press.

Plug, L.J., Werner, B.T., 2001. Fracture networks in frozen ground. J. Geophys. Res. 106, 8599–8613.

Plug, L.J., Werner, B.T., 2002. Nonlinear dynamics of ice-wedge networks and resulting sensitivity to severe cooling events. Nature 417, 929–932.

Pollard, W.H., French, H.M., 1980. A first approximation of the volume of ground ice, Richards island, Pleistocene MacKenzie delta, Northwest Territories, Canada. Can. Geotech. J. 17, 509–516.

Ray, R.J., Krantz, W.B., Caine, T.N., Gunn, R.D., 1983. A model for sorted patterned ground regularity. J. Glaciol. 29 (102), 317–337.

Russell, P.S., Head, J.W., Hecht, M.H., 2003. Evolution of volatile-rich crater interior deposits on Mars. In: 6th International Conference on Mars, Pasadena. Abstract 3256.

Schorghofer, N., Aharonson, O., 2003. Understanding the vertical distribution and exchange of water in the subsurface of Mars. In: AGU Fall Meeting. Abstract C21C-0828.

Schultz, R.A., Okubo, C.H., Wilkins, S.J., 2004. Displacement length scaling of faults on Earth, Mars and beyond. Lunar Planet. Sci. 35. Abstract 1157.

Seibert, N.M., Kargel, J.S., 2001. Small-scale martian polygonal terrain: implications for liquid surface water. Geophys. Res. Lett. 28 (5), 899–902.

Sletten, R.S., Hallet, B., Fletcher, R.C., 2003. Resurfacing time of terrestrial surfaces by the formation and maturation of polygonal patterned ground. J. Geophys. Res. 108 (E4), 25-1.

Smith, P.H., 2003. The Phoenix scout mission. In: 3rd Mars Polar Conference, Lake Louise. Abstract 8107.

Soare, R.J., Peloquin, C., 2003. Crater based evidence of periglacial processes in Northwest Utopia Planitia. Amer. Geophys. Un. Fall Meeting, San Francisco. Abstract C21C-0825.

Sullivan, R., Thomas, P., Veverka, J., Malin, M., Edgett, K., 2001. Mass movement slope streaks imaged by the Mars Orbiter Camera. J. Geophys. Res. 106 (E10), 23607–23627.

Swanson, D.K., Ping, C., Michaelson, G.J., 1999. Diapirism in soils due to thaw of ice-rich material near the permafrost table. Permafrost Periglac. 10, 349–367.

Thomas, P.C., 2003. The south polar residual cap of Mars: layers, erosion, and stratigraphy. In: 3rd Mars polar Conf., Lake Louise. Abstract 8047.

Thomas, P.C., Malin, M.C., Edgett, K.S., Carr, M.H., Hartmann, W.K., Ingersoll, A.P., James, P.B., Soderblom, L.A., Veverka, J., Sullivan, R., 2000. North–south geological differences between the residual caps on Mars. Nature 404, 161–164.

Titus, N.T., Kieffer, H.H., Christensen, P.R., 2003. Exposed water ice discovered near the south pole of Mars. Science 299, 1048–1051.

Tokano, T., 2003. Spatial inhomogeneity of the martian subsurface water distribution: implication from a global water cycle model. Icarus 164, 50–78.

Tokar, R.L., Feldman, W.C., Prettyman, T.H., Moore, K.R., Lawrence, D.J., Elphic, R.C., Kreslavsky, M.A., Head III, J.W., Mustard, J.F., Boynton, W.V., 2002. Ice concentration and distribution near the south pole of Mars: synthesis of odyssey and global surveyor analyses. Geophys. Res. Lett. 29 (19), 10-1.

Tsytovich, N.A., 1975. The Mechanics of Frozen Ground. McGraw–Hil, New York. 426 p.

Turcotte, D.L., Schubert, G., 1982. Geodynamics: Applications of Continuum Physics to Geological Problem. Wiley, New York.

Ugolini, F.C., Bockheim, J.G., Anderson, D.W., 1973. Soil development and patterned ground evolution in Beacon Valley, Antarctica. In: 2nd Int. Conf. on Permafrost, Yakoutsk, pp. 246–254.

Van Vliet-Lanoë, B., 1991. Differential frost heave, load casting and convection: converging mechanisms; a discussion of the origin of cryoturbations. Permafrost Periglac. 2, 123–139.

Van Vliet-Lanoë, B., 1998. Frost and soils: implications for paleosols, paleoclimates and stratigraphy. Catena 34, 157–183.

Walker, D.A, Walker, M.D., Everett, K.R., Webber, P.J., 1985. Pingos of the Prudhoe Bay region, Alaska. Arctic Alpine Res. 17 (3), 321–336.

Walker, D.A., Epstein, H.E., Gould, W.A., Kade, A.N., Kelley, A.M., Knudson, J.A., Krantz, W.B., Michaelson, G., Peterson, R.A., Ping, C., Raynolds, M.K., Romanovsky, V.E., Shur, Y., Walker, M.D., 2003. Biocomplexity of frost-boil ecosystems: a conceptual model of frost-boil

development in relationship to vegetation along the Arctic bioclimate gradient. Permafrost Periglac. Submitted for publication.

Washburn, A.L., 1956. Classification of patterned ground and review of suggested origins. Geol. Soc. Am. Bull. 67, 823–865.

Werner, B.T., Hallet, B., 1993. Numerical simulations of self-organized stone stripes. Nature 361, 142–144.

Wyatt, M.B., McSween Jr., H.Y., Christensen, P.R., Head III, J.W., 2003. Basalt, altered basalt, and andesite on the martian surface: observations, interpretations, and outstanding questions. In: 6th Int. Conf. on Mars, Pasadena. Abstract 3271.

Yoshikawa, K., 2002. Origin of the polygons and underground structures in Western Utopia Planitia on Mars. Lunar Planet. Sci. 33. Abstract 1159.